

Citation

Cheng, R. and Chen, W. and Hao, H. and Li, J. 2021. A state-of-the-art review of road tunnel subjected to blast loads. *Tunnelling and Underground Space Technology*. 112: ARTN 103911. <http://doi.org/10.1016/j.tust.2021.103911>

1 **A state-of-the-art review of road tunnel subjected to blast loads**

2 Ruishan Cheng, Wensu Chen^{*}, Hong Hao^{*}, Jingde Li

3 *Center for Infrastructural Monitoring and Protection, School of Civil and Mechanical Engineering, Curtin*
4 *University, Australia*

5 ^{*}Corresponding authors: wensu.chen@curtin.edu.au (Wensu Chen), Hong.Hao@curtin.edu.au (Hong Hao)

6 **Abstract:** Road tunnels are critical components in road transportation networks. In their service life
7 they may subject to explosion loads from terrorist bombing attacks, engineering blasting for
8 construction and accidental explosions from transported flammable goods. These extreme loading
9 conditions might not only lead to catastrophic damages to tunnel structures, severe casualties and
10 economic losses, but also have immeasurable social impacts. Therefore, it is imperative for engineers,
11 researchers and policy regulators to understand the performance of road tunnels under explosion loads
12 towards a reliable blast-resistant design of tunnel structures. This paper presents a state-of-the-art
13 review of dynamic response, damage assessment and damage mitigation of tunnels under blast loads.
14 The common road tunnels, various explosion scenarios, and the corresponding blast wave
15 characteristics are reviewed first. Then the dynamic response and damage characteristics of tunnel
16 structures under blast loads including the analysis methods of tunnel response, types of tunnel
17 response and key factors influencing tunnel response are reviewed and discussed. The assessment
18 criteria of tunnel damage and the damage mitigation measures for tunnels against blast loads are also
19 reviewed. Finally, concluding remarks and several key research areas for future work are presented.
20 **Keyword:** Road tunnel, explosion, blast response, damage assessment, damage mitigation

21 **1. Introduction**

22 Road tunnels, either buried, underground, under river or even subsea tunnels, are usually
23 constructed as an important part of modern highway network to shorten the travel time within or
24 between cities, reduce transportation costs, and improve traffic capacity (Cui, et al., 2015, Wang, et
25 al., 2020). Based on open reports and literature, **Figure 1** (a) and (b) summarize the total number and
26 mileage of road tunnels, respectively. By 2019, China has built 19067 road tunnels with the total
27 mileage of 18966.6 km (MTPRC, 2020). With the foreseeable growth of transportation demand, road
28 tunnels will be more intensively constructed worldwide and play increasingly vital roles in the
29 transportation systems by virtue of its great advantage in overcoming physical barrier and minimizing
30 local environment impact (Bassan, 2015).

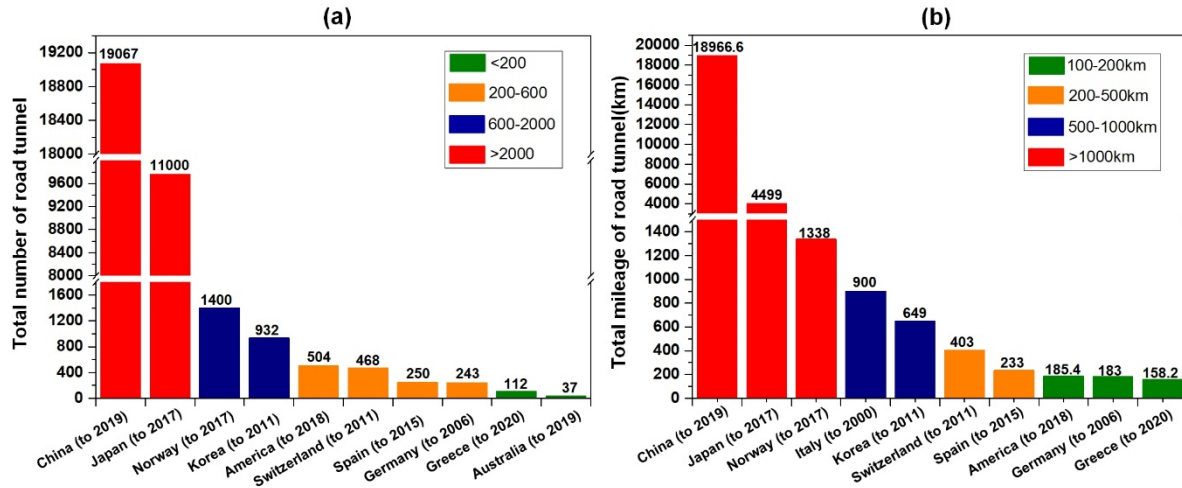


Figure 1. The total number and mileage of road tunnels. (a) the number of road tunnels, and (b) the mileage of road tunnels.

31

32

33

34

35

36

37

38

39

40

41

42

43

44

45

46

47

48

49

50

51

52








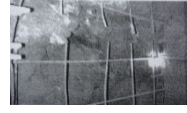
53

54

Road tunnels described as “traffic throats” or “choke points” are usually buried in various media (e.g. rock, soil and water) and are therefore in enclosed environment to connect open-air highway at both ends (TCRP86/NCHRP525, 2006). Some unexpected damage to a road tunnel can significantly and adversely affect or even disrupt the surrounding transportation network linked by the road tunnel. Hence, the safety issue of road tunnels has drawn more and more attentions from the local authorities to federal governments (Roberts, et al., 2003). During service life, road tunnels might be subjected to terrorist attacks, accidental explosions such as the explosion of transported flammable goods, or the blasting due to adjacent construction excavations, which might result in severe casualties, irreversible damage to tunnel structures and facilities. As reported by Masellis, et al. (1997), a tank-truck carrying 2500 litres of liquid petroleum gas (LPG) was hit by a coach car in a tunnel along the Palermo-Punta Raisi motorway (Italy) in March 1996, leading to a boiling liquid expanding vapour explosion (BLEVE) that caused 5 deaths, 34 injuries and severe damage to tunnel structures. It was also reported by Ingason and Li (2017) that a rear-end collision accident involving two methanol tankers occurred inside the Yanhou tunnel of China in 2014, inducing an explosion of a liquid methoxymethane tanker inside the tunnel 100 m from the entry portal. The explosion led to 52 casualties and destroyed 42 vehicles inside the tunnel. Some major accidental explosion accidents including BLEVE, Vapour Cloud Explosion (VCE) and high explosive (HE) blasting attacks from terrorists inside or in the vicinity of tunnels are listed in **Table 1**. Although it is seen in **Table 1** that the majority of terrorist attacks occurred in subway tunnels, many key road tunnels for the connections of adjacent important economic regions are also tempting attack targets, since the disruption of the road tunnels can hinder fluent cargo transportation and economic flows for a long time.

Table 1. Tunnel explosion incidents

Explosion type	Year	Name of Tunnel	Country	Cause	Consequence		Accident scene
					Casualties	Tunnel damage	
Boiling Liquid Expanding Vapor Explosion (BLEVE)	1982 (Bangash and Bangash, 2005)	Salang tunnel	Afghanistan	Fuel truck explosion	1000-3000 deaths	Severe tunnel damage	 From (1) below
	1996 (Masellis, et al., 1997)	Palermo-Punta Raisi tunnel	Italy	LPG truck hit	5 deaths, 30 injuries	Severe tunnel damage	
	1999 (Auboyer, et al., 2007)	The Tauern tunnel	Austria	Fuel truck explosion	12 deaths, 48 injuries	Severe tunnel damage	
	2007 (McDaniel, 2017)	Newhall Pass Tunnel	United States	Car collision	2 deaths, 10 injuries	Severe tunnel damage (small explosion may occur)	
	2007 (Dix, 2012)	Burnley tunnel	Australia	Vehicle collision	3 deaths	Local tunnel damage	
	2011 (Lai, et al., 2016)	Qidaolia ng tunnel	China	Truck tanker explosion	4 deaths, 1 injuries	Severe tunnel damage, local collapse	
	2012 (From (2) below)	Dimuan tunnel	China	Truck tanker explosion	5 deaths	Slight tunnel damage	
	2014 (Li, 2018)	Yanhou tunnel	China	Methanol vehicle collision	40 deaths, 12 injuries	Severe tunnel damage	
2015 (From (3) below)	Skatestr aum tunnel	Norway	Fuel truck trailer crashing into wall	-	Severe tunnel damage		
Vapor Cloud Explosion (VCE)	1993 (Nagao, et al., 1997)	Road tunnel in Tokyo	Japan	Methane leak from surrounding	4 deaths	NA	NA

	2005 (He, et al., 2019)	Dongjias han tunnel	China	Methane leak from surroundin g	44 deaths, 11 injuries	Severe tunnel deformation	
	2015 (He, et al., 2019)	Wuluolu tunnel	China	Methane leak from surroundin g	7 deaths, 19 injuries	Severe tunnel collapse	
	2017 (He, et al., 2019)	Qishany an tunnel	China	Methane leak from surroundin g	12 deaths, 12 injuries	Severe tunnel collapse	
Highly- explosive Explosion (HE)	2005 (From (4) below)	London subway tunnel	British	Bomb attack	52 deaths, 700 injuries	Severe tunnel damage	
	2010 (Li, 2018)	Moscow metro Tunnel	Russia	Bomb attack	41 deaths, 120 injuries	Severe tunnel damage	
	2011 (From (5) below)	Minsk Metro tunnel	Belarus	Bomb attack	12 deaths, over 200 injuries	Severe tunnel damage	
	2012 (From (6) below)	Yanru tunnel	China	Highly- explosive explosion	20 deaths, 2 injuries	Severe tunnel damage	
	2012 (Yan, et al., 2019)	Lvliang tunnel	China	Highly- explosive explosion	8 deaths, 5 injuries	Severe tunnel damage	

56 Note: website (1):<https://devastatingdisasters.com/salang-tunnel-fire-1982/>;
57 (2):<http://hunan.sina.com.cn/news/b/2012-10-07/081019665.html>;
58 (3):<https://www.youtube.com/watch?v=vqt-cC3Y4OU>;
59 (4):<https://www.mylondon.news/news/nostalgia/gallery/pictures-look-back-77-london-18555867>;
60 (5):<https://www.youtube.com/watch?v=KWE2aGdpNuo>;
61 (6): http://www.china.com.cn/news///node_7153238.htm

62 The blast-resistant capacity of reinforced concrete (RC) lining structures of road tunnels is of
63 great significance to prevent road tunnels from the fatal damage under intensive explosion loads.
64 However, the existing design guidelines or manuals of road tunnels, as listed in **Table 2**, barely
65 consider the effect of explosion loads on structural response despite intensive damages to many
66 tunnels as partially listed in Table 1. Some design guides such as UFC 3-340-02 (US Department of

67 Defense, 2008) and ASCE/SEI 59-11 (ASCE, 2011) provide design guidelines and recommendations
 68 for the blast resistance of RC structures for buildings and bridges. It should be noted that the response
 69 of RC tunnel structures subjected to blast loads is more complex owing to the interaction between the
 70 buried tunnel structure and its surrounding media (Weidlinger and Hinman, 1988). So far, designers
 71 and engineers of road tunnels still lack necessary guideline to estimate the vulnerability of tunnel
 72 structures under explosion loads although some research works have been carried out and results
 73 reported in literature. This paper presents a comprehensive review of the existing literature on the
 74 dynamic response, damage assessment and damage mitigation of tunnels subjected to explosion loads,
 75 which will help researchers and tunnel engineers to better understand the current research status and
 76 understanding of the dynamic behaviours of road tunnels subjected to explosion loads.

77 **Table 2.** Design guidelines and manuals of road tunnels.

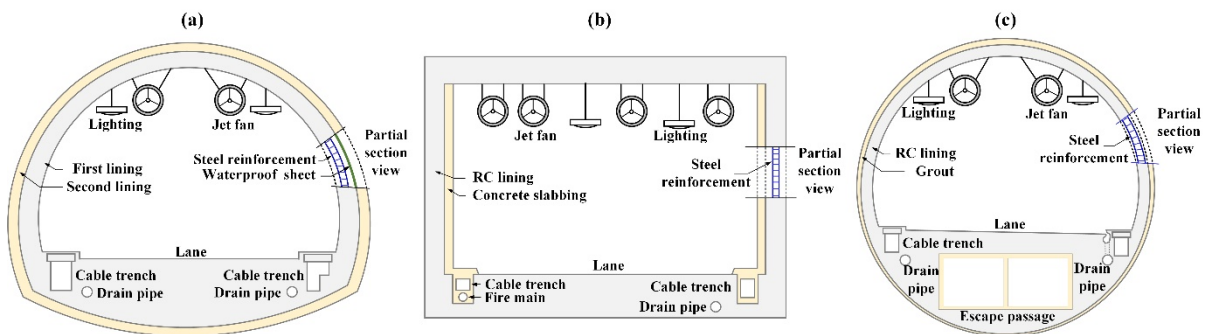
Guideline	Country	Agency	Remarks
Design Criteria for Bridges and Other Structures. Part C: Tunnels (DTMR, 2020)	Australia	Department of Transport and Main Roads	Static loads, fire and heat loads, traffic loads, etc.
Guide to Road Tunnels. Part 2: Planning, Design and Commissioning (Austroads, 2019)	Australia and New Zealand	Austroads	Static loads, fire and heat loads, traffic loads, seismic loads, etc.
Specifications for Design of Highway Tunnels Section 1 Civil Engineering (MTPRC, 2018)	China	Ministry of Transport of the People's Republic of China	Static loads, structural loads, heat loads, frost heave forces, seismic loads, etc.
Technical Standard for Structure Design of Road Tunnel (JRA, 2003)	Japan	Japan Road Association	Static loads, traffic loads, seismic loads, etc.
Guideline for Design of Road Tunnel (RDA and JICA, 2018)	Japan	Japan International Cooperation Agency	Static loads, seismic loads, traffic loads, etc.
(Manual 021) Road Tunnels (NPRA, 2004)	Norway	Norwegian Public Road Administration	Static loads, wind loads, fire loads, frost loads, etc.
Design Manual for Roads and Bridges, Part 9, Section 2 of Volume 2, Design of Road Tunnels (UKHA, 2000)	United Kingdom	UK Highways Agency	Static loads, traffic loads, fire loads, etc.
Tunnel lining design guide (BTSICE, 2004)	United Kingdom	The British Tunnelling Society and The Institution of Civil Engineers	Static loads, seismic loads, fire loads, temporary construction loads, etc.
FHWA Road Tunnel Design Guidelines (USDTFHA, 2004)	United States	U.S. Department of Transportation Federal Highway Administration	Static loads, construction load, seismic load, fire loads, etc.

78

79 This review paper summarizes the current research status and recent advances on the road tunnels
80 subjected to explosion loads. The structure of this paper is organized as follows: Firstly, the common
81 road tunnels, various explosion scenarios, and the corresponding blast wave characteristics are
82 reviewed in Section 2 and 3. Next, dynamic response and damage of tunnel subjected to blast loads
83 involving the analysis methods of tunnel response, types of tunnel responses, and key factors
84 influencing tunnel responses are included in Section 4. Then, the assessment criteria of tunnel damage
85 are summarized in Section 5, followed by damage mitigation measures for tunnels against blast loads
86 in Section 6. At last, concluding remarks and several necessary key research areas for future work are
87 presented in Section 7.

88 2. Overview of common road tunnels

89 A typical road tunnel consists of the main body tube and the portal of tunnel. **Figure 2** shows
90 three typical cross sections of the main body tube. Their advantages, disadvantages and applicable
91 geological conditions are summarized in **Table 3**. In the longitudinal direction, the portals at both
92 ends of the road tunnel might extend outward a certain distance from the buried medium and expose
93 to free air, while the main body tube of the road tunnel is usually buried in different media, i.e., rock
94 mass, soil and water. Accordingly, road tunnels could be divided into three categories, i.e., tunnels in
95 rock mass, tunnels in soil and tunnels under water. Meanwhile, the road tunnels under water can be
96 further divided into two categories, i.e., tunnels in water (tunnels submerged or floated in water or
97 the bottom of water) and tunnels below water (tunnels buried in soil or rock mass under water). It
98 should be noted that one tunnel might run across different buried media. As reported in Shirlaw, et
99 al. (2000) and Zhao, et al. (2007), both Kranji tunnel and the tunnel along North East line in Singapore
100 run across rock mass and soil along their respective routes.



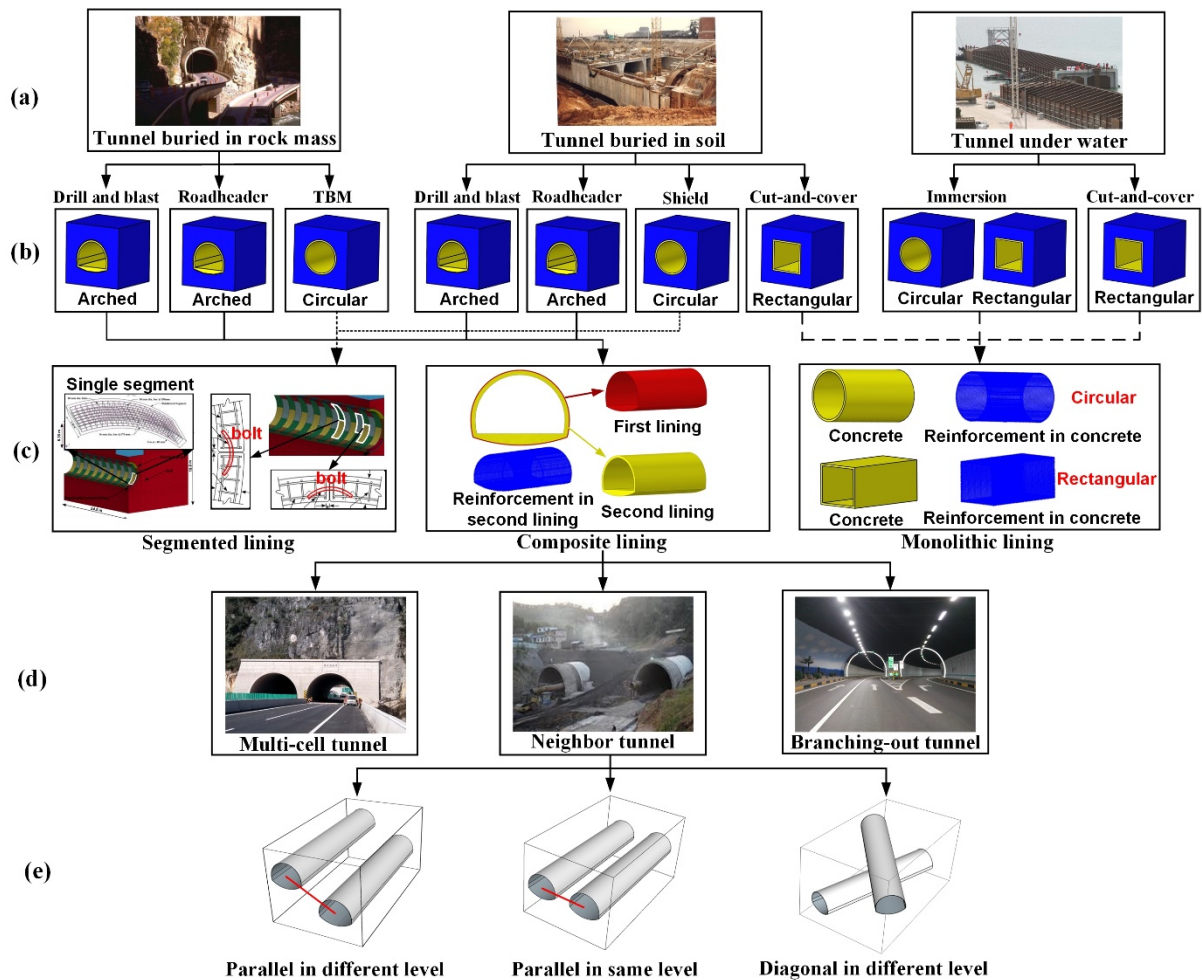
101

102 **Figure 2.** Typical cross sections of road tunnel with (a) arched shape, (b) rectangular shape, and (c) circular shape.

103 **Table 3.** Summary of typical three cross sections of tunnel

Cross section	Advantage	Disadvantage	Applicable geological conditions	Ref.
Rectangular	High utilization rate of inner space as traffic tunnel	Poor self-stability and weak resistance to surrounding pressure	Shallow soil layer with low static pressures	(AASHTO, 2012, USDTFHA, 2009)
Circular	Good self-stability, low ground settlement	Low utilization rate of inner space as traffic tunnel	Shallow buried soil near dense buildings, deep buried soil and rock mass with high overlying and side pressures	
Arched	Moderate self-stability with moderate inner utilization rate	Low resistance to high side pressures of tunnel surroundings	Deep buried soil and rock mass with high overlying pressures and moderate or low side pressures	

104 According to the design manuals of road tunnel in **Table 2**, road tunnels in different media, i.e.,
 105 rock mass, soil and water are usually excavated by using their respective favourite excavation
 106 methods and thus different cross section shapes are formed. The details are showed in **Figure 3(a)**
 107 and (b). As shown in **Figure 3(c)**, three lining types, i.e. segmental lining, composite lining and
 108 monolithic lining are correspondingly selected for road tunnels depending on the used excavation
 109 methods. The segmental lining consists of single segment and connecting joints between segments,
 110 where the single segment is composed of RC material. The composite lining mainly comprises the
 111 first lining and the secondary lining, where the first lining is usually composed of shotcrete with
 112 anchors and rebar nets, and the second lining normally consists of RC material. Meanwhile, the
 113 monolithic lining is composed of RC materials. In urban or suburb areas, due to the limitation of
 114 underground space, the neighbour tunnel, multi-cell tunnel and branching-out tunnel are commonly
 115 seen (see **Figure 3(d)**). For the neighbour tunnel, based on the relative positions of two tunnels, they
 116 can be categorised into three types, i.e., parallel tunnels at different levels, parallel tunnels at the same
 117 level and diagonal tunnels at different levels (see **Figure 3(e)**).



118

119

120

121

Figure 3. Summary of common road tunnels. (a) road tunnels buried in different media (Photos from USDTFHA (2009)), (b) excavation methods and cross-section shapes of road tunnels, (c) lining forms of road tunnels, (d) special forms of tunnel layouts, and (e) different layout forms for neighbour tunnels

122

3. Overview of possible explosion threats to tunnels

123

3.1. Explosion threat categories

124

125

126

127

128

129

The explosion threats to road tunnels during operation mainly result from three different sources, i.e., accidental explosions of flammable materials (e.g. flammable gas and volatile pressurized liquid) during transportation, terrorism or military bombing and construction blasting from adjacent site. Since these explosions may occur inside or in the vicinity of road tunnels, the explosions can be divided into two categories, i.e. internal and external explosions (see **Figure 4**) depending on the explosion locations.

130

131

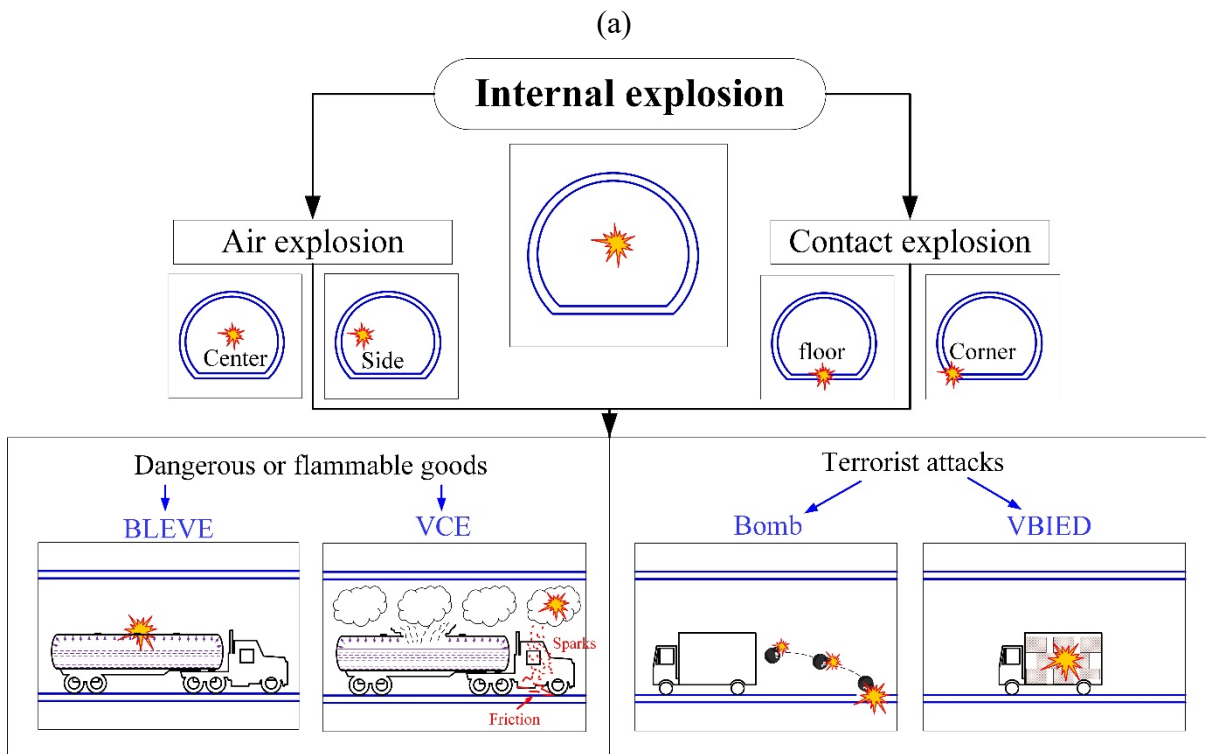
132

As shown in **Figure 4(a)**, the internal explosions can be further divided into internal air explosion (i.e. explosion in the air space of road tunnels) and internal contact explosion (i.e. close-in explosion on the wall or surface of road tunnels). Compared to the engineering blasting, the explosion of

133 flammable materials and terrorist attacks are more likely to cause internal explosions. For instance,
 134 if a tanker truck carrying flammable materials (e.g., Liquefied Natural Gas (LNG) and Liquefied
 135 Petroleum Gas (LPG)) collides with another vehicle, or hits tunnel wall, the internal explosions of
 136 boiling liquid expanding vapour explosion (BLEVE) and vapour cloud explosion (VCE) are very
 137 likely to be triggered. In addition, with the rising terrorism activities, road tunnels are also confronted
 138 with the potential threats from improvised explosive devices such as the vehicle-borne improvised
 139 explosive devices (VBIEDs) and the suitcase bombs.

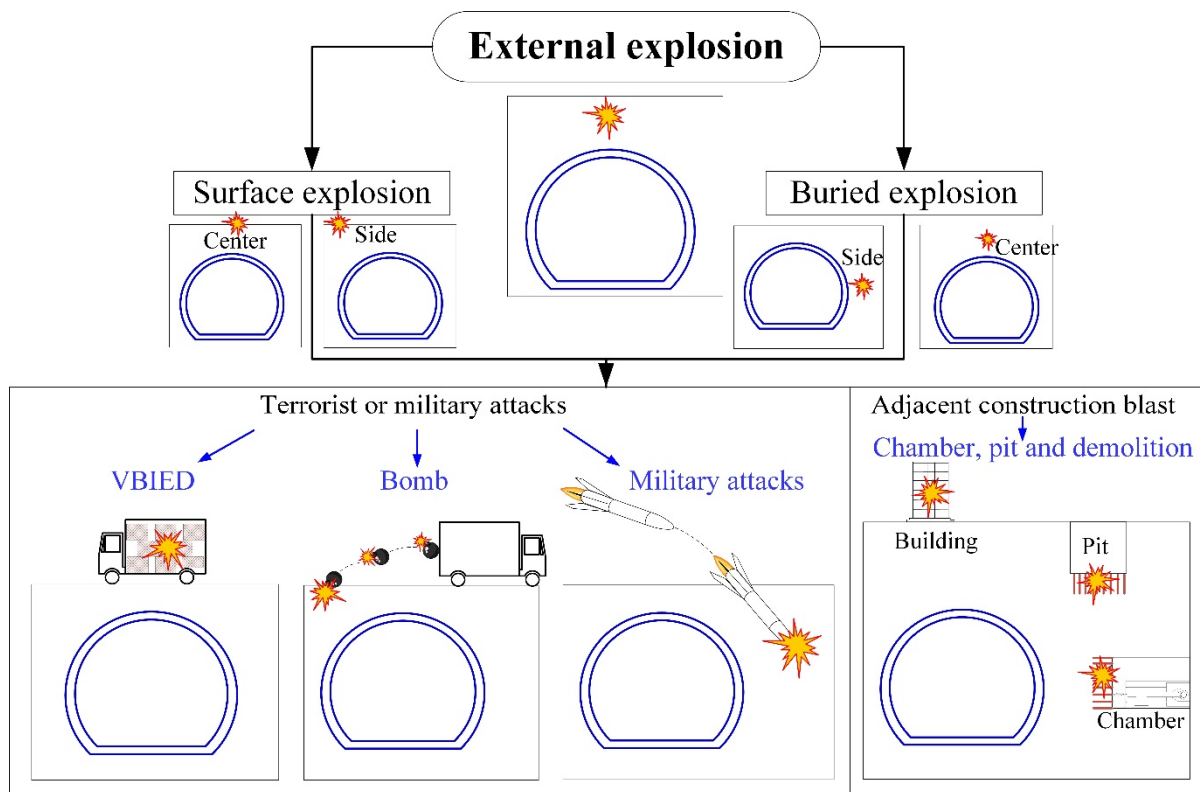
140 As shown in **Figure 4(b)**, the external explosions can be subdivided into external surface
 141 explosions (i.e., explosions on the ground near road tunnels) and external buried explosions (i.e.
 142 explosions in buried media near road tunnels). In city, terrorist attacks are more likely to occur on or
 143 near the ground surface of tunnels, thereby being deemed as the external surface explosions of
 144 shallow urban road tunnel. Meanwhile, road tunnels may face the threats of hostile military attacks,
 145 where most missiles could penetrate the ground and explode below ground surface to result in external
 146 buried explosions. In addition, the engineering blasting, such as the demolition blasting of adjacent
 147 building, or the blasting excavations of urban foundation pit and underground chamber near existing
 148 road tunnels, might act as external surface explosion or buried explosion that can potentially threaten
 149 road tunnels.

150



151

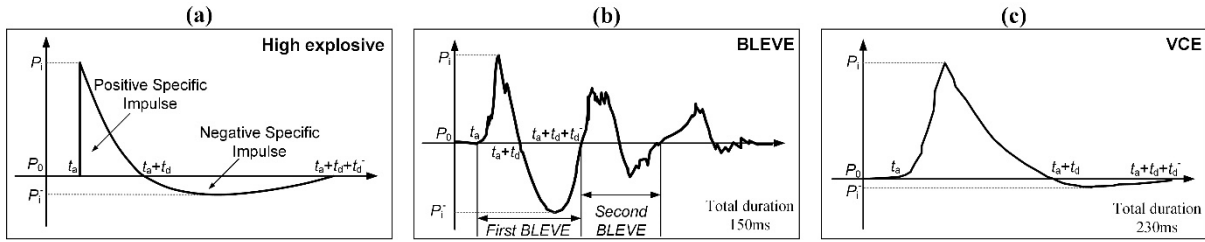
152



153
154 **Figure 4.** Types of explosions threaten road tunnels. (a) internal explosion, and (b) external explosion.

155 **3.2. Characteristics of explosion pressure and blast wave around**
156 **tunnels**

157 Terrorist bombing, military attacks and engineering blasting are mostly associated with high
158 explosives, whereas gas explosions are resulted from gaseous material with slower chemical reaction
159 than that of high explosives. Therefore, compared to high explosives, the blast waves generated by
160 gas explosions are different (Birk, 2017). As shown in **Figure 5**, the high explosive generates much
161 steeper blast wave than gas explosion. The pressure of high explosive instantaneously increases to
162 the peak incident pressure P_i (as seen in **Figure 5** (a)), while the blast waves of gas explosions (as
163 seen in **Figure 5** (b) and (c)) gradually increase to the maximum pressure P_i . In order to further
164 illustrate the difference between high explosive explosion and gas explosion, the characteristics of
165 the BLEVE loading in **Figure 5**(b) and its TNT equivalent loading characteristics are compared in
166 **Table 4**. Gas explosions usually generate blast waves with lower peak overpressures but longer
167 duration and higher impulses than those of high explosive explosion with the same TNT equivalency
168 (Hao, et al., 2016). Compared to high explosive explosion, the lower peak pressure and slower rising
169 time of gas explosion can reduce the instantaneous shear stress in tunnel structures and the risk of
170 crushing damage on tunnel structures, while the longer duration and higher impulsive are prone to
171 induce severe bending deformation and thus increase the risk of tensile damage.



172

173

174

175

176

177

Figure 5. Typical blast loads from (a) high explosive (US Department of Defense, 2008), (b) BLEVE (Birk, et al., 2007), and (c) VCE (CCPS, 2010), respectively. P_0 represents the ambient pressure. P_i , and P_i^- , represent the maximum positive and negative peaks of incident pressure, respectively. t_a , t_d , and t_d^- represent the arrival time of incident wave, the positive duration of wave, and the negative duration of wave, respectively.

Table 4. The blast loading characteristics of gas explosion and high explosive explosion

Explosion type	Peak pressure	Rising time	Positive duration	Negative duration	Total duration
Gas explosion	About 9 kPa	About 12 ms (First BLEVE)	About 38 ms (First and second BLEVE)	About 45 ms (First and second BLEVE)	About 83 ms (First and second BLEVE)
High explosive explosion	About 14 kPa	Almost instantaneous	About 10 ms	About 28 ms	About 38 ms

178

Note: TNT equivalent loading characteristics are obtained based on UFC 3-340-02 (US Department of Defense, 2008)

179

180

181

182

183

184

185

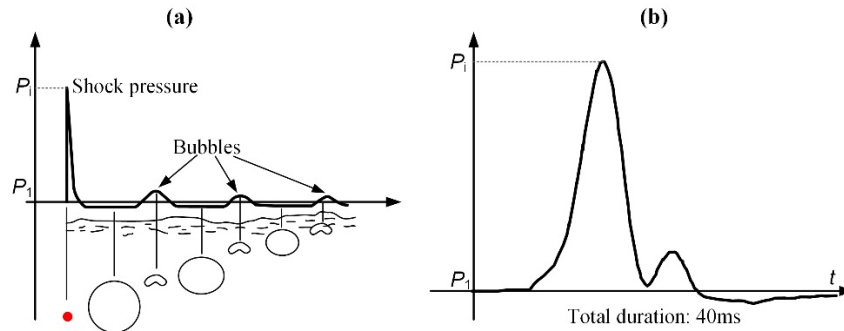
186

187

188

189

The blast loads acting on tunnel structures could be generated in different media such as air, soil, and water, etc. The characteristics of blast loads in different media are different. Taking the high explosive as an example, the blast load in air domain has the profile as shown in **Figure 5(a)** (US Department of Defense, 2008), while the blast loads in water consist of shock front followed by a series of pressure pulses which are caused by subsequent oscillations of bubbles (Wang, et al., 2020), as shown in **Figure 6(a)**. The blast load in the solid medium (soil or rock mass) could rise quickly near the explosion source, similar to the blast load in air (Vivek and Sitharam, 2018). However, as the shock front propagates in the solid media, it rapidly attenuates to a lower intensity stress wave with a gradual decrease in peak pressure (Vivek and Sitharam, 2017). A typical pressure time history of blast load with a non-instantaneous rise in solid medium can be found in Lu, et al. (2005), as shown in **Figure 6(b)**.



190
191
192

Figure 6. Blast pressure-time histories in (a) water (Swisdak Jr, 1978), and (b) solid medium (Lu, et al., 2005). P_i is the positive peak pressure, P_1 is the ambient pressure.

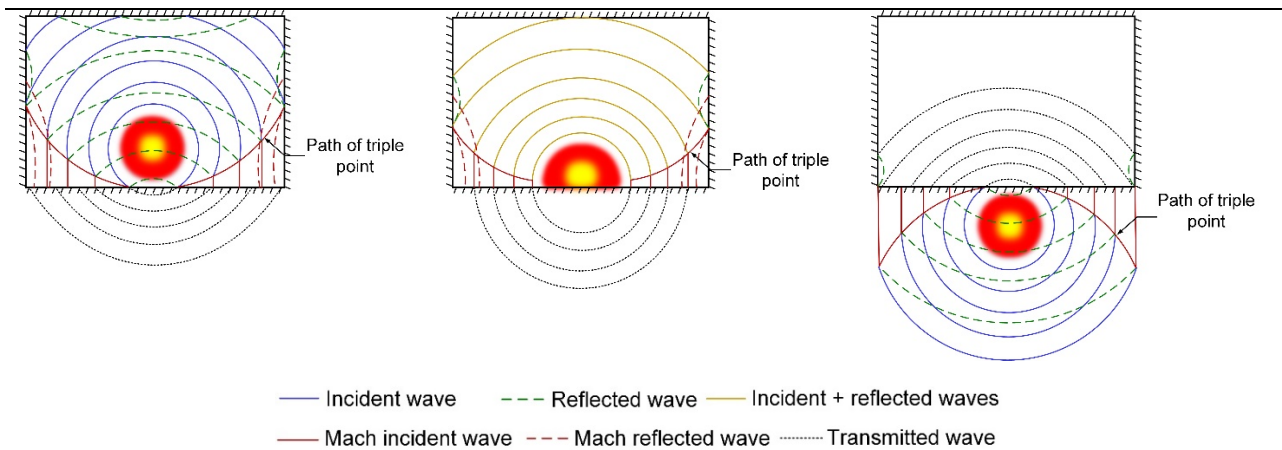
193
194
195
196
197
198
199
200
201
202
203
204
205
206
207
208
209
210
211
212

When the explosion occurs inside or outside the tunnel, the reflected and transmitted blast waves interact each other. A rectangular tunnel is taken as an example to illustrate the behaviours of blast waves inside and around the tunnel under internal and external explosions, as shown in **Table 5**. For the scenario of internal air explosion, when initial blast incident waves encounter the closest tunnel wall, the reflected and transmitted blast waves are formed simultaneously. The reflected blast waves continue to propagate in the tunnel, and the transmitted blast waves continue to propagate outwards in the medium around tunnel. When the reflected blast waves reach the other sides of tunnel wall, the reflected waves re-reflect again, thereby resulting in multiple pressure peaks inside the tunnel. In addition, Mach fronts could be also formed at the closest tunnel wall due to the interaction of the initial blast waves with the reflected blast waves. As Mach waves continue to propagate along the tunnel wall and to impinge other tunnel walls, the reflected Mach waves may be formed. For the scenario of internal contact explosion, the generated Mach waves are similar with the Mach waves of internal air explosion. However, unlike the internal air explosion, the reflected waves from the internal contact explosion merge with the incident waves at the point of detonation source to form single waves with hemispherical shape, which yields higher blast pressure and impulse. For the scenario of external explosion, when the initial blast waves arrive at the closest tunnel wall, most blast waves are reflected into surrounding medium and only a small portion of blast waves are transmitted into the inner tunnel. Although the transmitted waves continue to propagate and reflect in tunnel, the damage of the transmitted wave to tunnel could be negligible due to the low loading intensity.

213

Table 5. Blast wave propagation inside and in the vicinity of tunnels

Internal air explosion	Internal contact explosion	External explosion
------------------------	----------------------------	--------------------



214 **4. Response and damage of tunnel subjected to explosion load**

215 **4.1 Analysis methods of tunnel response under explosion**

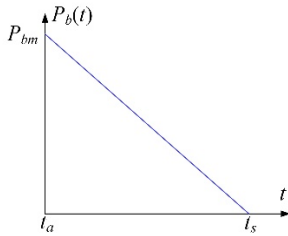
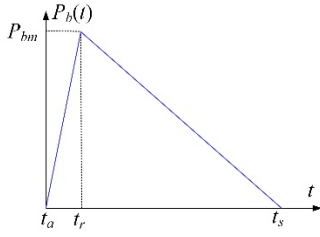
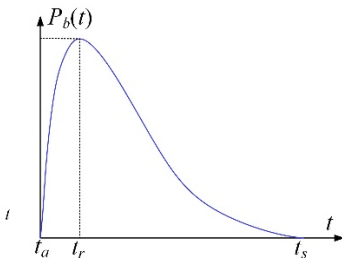
216 Analysis methods of tunnel responses under explosions can be divided into three categories, i.e.,
 217 theoretical methods, experimental methods, and numerical methods, as described below.

218 **4.1.1 Theoretical methods**

219 Three analytical methods based on Fourier transform (Li and Li, 2018, Li, et al., 2018, 2020, Tao,
 220 et al., 2019), Laplace transform (Gao, et al., 2013, Senjuntichai and Rajapakse, 1993), and modal
 221 superposition (Chen, et al., 2013a, 2013b, Ma, et al., 2010) to investigate the tunnel response under
 222 blast loads could be found in the literature. Two forms of blast loads, i.e., simplified triangular loads
 223 (e.g., right and non-right) and equivalent exponential loads were commonly used in the analytical
 224 methods. Their expressions are given in **Table 6**. The governing formulae, advantages, and
 225 shortcomings of three analytical methods are summarized in **Table 7**. The first analytical method
 226 based on the Fourier transform technique could convert the steady-state response of tunnels under
 227 harmonic waves into the transient response of tunnels subjected to blast loads by using Fourier
 228 transform and its inversion. The second analytical method based on the Laplace transform first
 229 calculates the transient response of tunnel in Laplace domain. The solution in Laplace domain is then
 230 converted into time domain by the inverse Laplace transform. In the existing studies, the Fourier
 231 transform technique was commonly used to solve the transient response of unlined tunnel (i.e.,
 232 without the lining-surroundings interaction) against external explosions, while the Laplace transform
 233 was often employed to analyze the dynamic response of lined tunnel (i.e., with lining-surroundings
 234 interaction) subjected to internal explosions. In fact, both Fourier transform and Laplace transform
 235 techniques can be applied to study the dynamic response of tunnels subjected to internal explosion
 236 and external explosion scenarios with or without lining-surroundings interaction. The challenges are

237 that the direct inversions of Fourier transform and Laplace transform are usually difficult or
 238 sometimes not available owing to complex integral paths and possible singularity during inversion.
 239 Accordingly, the algorithms such as the Trapezoidal Approximation technique (Li, et al., 2018) for
 240 Fourier transform and the Durbin's formula (Gao, et al., 2013) for Fourier transform and the Durbin's
 241 formula (Gao, et al., 2013) for Laplace transform are developed to numerically solve the inversions
 242 in order to obtain approximate results. Unlike the above two methods, the analytical method based
 243 on modal superposition does not require the difficult inversion procedure and solves the transient
 244 response of tunnel against explosions with the superposition of various modal response results.
 245 However, high-order modal results of tunnel structural response are usually neglected in this
 246 analytical method for fast and easy calculation. Hence, the accuracy of this analytical solution is also
 247 limited.

248 **Table 6.** The most used blast loading types in analytical methods of dynamic response of tunnel

Blast loading types	Graphs	Equations	Ref.
Simplified right triangular load		$P_b(t) = \begin{cases} 0 & , t < t_a \\ \frac{t_s - t}{t_s - t_a} P_{bm} & , t_a \leq t < t_s \\ 0 & , t_s \leq t \end{cases}$	(Ma, et al., 2010)
Simplified non-right triangular load		$P_b(t) = \begin{cases} 0 & , t < t_a \\ \frac{t}{t_r - t_a} P_{bm} & , t_a \leq t < t_r \\ \frac{t_s - t}{t_s - t_r} P_{bm} & , t_r \leq t < t_s \\ 0 & , t_s \leq t \end{cases}$	(Li, et al., 2018)
Equivalent exponential load		$P_b(t) = \begin{cases} 0 & t < t_a \\ e^{\frac{\alpha}{\beta} \arctan\left(\frac{\beta}{\alpha}\right) \sqrt{1 + \left(\frac{\beta}{\alpha}\right)^2}} \cdot e^{-\alpha t} \sin \beta t & \alpha \geq 0, t_a \leq t < t_r \\ e^{\frac{\alpha}{\beta} \left(\arctan\left(\frac{\beta}{\alpha}\right) + \pi\right) \sqrt{1 + \left(\frac{\beta}{\alpha}\right)^2}} \cdot e^{-\alpha t} \sin \beta t & \alpha \leq 0, t_r \leq t < t_s \\ 0 & t_s \leq t \end{cases}$	(Tao, et al., 2019)

249 **Note:** $P_b(t)$ represents the blast loading time history, P_{bm} is the peak pressure of the blast loading, t_a , t_r and t_s are the arrival
 250 time, the rising time and total time of the blast loading, respectively. Where β is equal to π / t_s , α is determined by
 251 $\beta \cot \beta t_r$.

252 **Table 7.** Summary of three analytical methods

Method	Key governing formulae	Advantage	Disadvantage
Based on Fourier transform	$g(H_i, t) = \frac{1}{\sqrt{2\pi}} \int_{-\infty}^{+\infty} \chi(H_i, \omega) F(\omega) e^{-i\omega t} d\omega$ $g(H_i, t): \text{The transient response of tunnel}$ $\chi(H_i, \omega): \text{The steady-state response of tunnel with a specific frequency } \omega$ $F(\omega): \text{Transformed Fourier form of blast load}$	Bridging the gap between the steady-state and transient response	Complex integral paths, difficult direct inversion of Fourier transform
Based on Laplace transform	$\frac{\partial^2 \bar{\varphi}}{\partial r^2} + \frac{1}{r} \frac{\partial \bar{\varphi}}{\partial r} = \frac{s^2}{c^2} \bar{\varphi}$ $s: \text{Transform parameter}$ $c: \text{Propagation speed of blast wave in medium}$ $r: \text{Travel distance of blast wave in medium}$ $\bar{\varphi}: \text{Laplace transform of potential function } \varphi \text{ of displacement}$	Using transform function to reduce the difficulty of solving differential equation	Difficult or sometimes not available for direct inversion of Laplace transform
Based on modal superposition	$w(x, t) = \sum_{n=1}^{+\infty} W_n(x) q_n(t)$ $w(x, t): \text{The transient response of tunnel}$ $W_n(x): \text{The } n^{\text{th}} \text{ mode shape}$ $q_n(t): \text{The } n^{\text{th}} \text{ generalized modal coordinate}$	Not requiring complex inversion	Simple linear superimposition, usually only superimposing several low-order modal results

253 The intensities of shock and stress waves induced by close-in explosions usually far exceed the
254 strength of tunnel structures, causing plastic response of tunnel structures. However, the above three
255 analytical methods for the tunnel response under blast loads are based on the theory of elastic wave.
256 Hence, the analytical solutions derived by the elastic wave theory are not suitable for the response
257 analysis of tunnel structures subjected to close-in explosions. Moreover, both tunnel and buried media
258 material need be homogeneous and isotropic in the analytical methods, whereas the concrete and
259 surrounding media around tunnel are actually heterogeneous. Hence, the aforementioned analytical
260 solutions do not necessarily give accurate predictions of blast response of tunnel.

261 4.1.2 Experimental methods

262 Experimental methods including field and laboratory tests are another approaches to investigate
263 the dynamic response and damage of tunnel structural elements under explosion loads. The
264 experimental tests can be classified into two categories based on the model size, i.e., the full-scale
265 tests and the scaled-down tests. **Table 8** summarizes some typical experimental tests of the tunnel
266 responses under blast loads. Test methods, test instruments in experiments, and their corresponding
267 advantages and disadvantages are summarized in **Table 9**.

268 For internal explosions in tunnel, limited full-scale tests have been conducted to investigate the
269 behaviour of tunnels subjected to explosion loads. One representative internal full-scale explosion

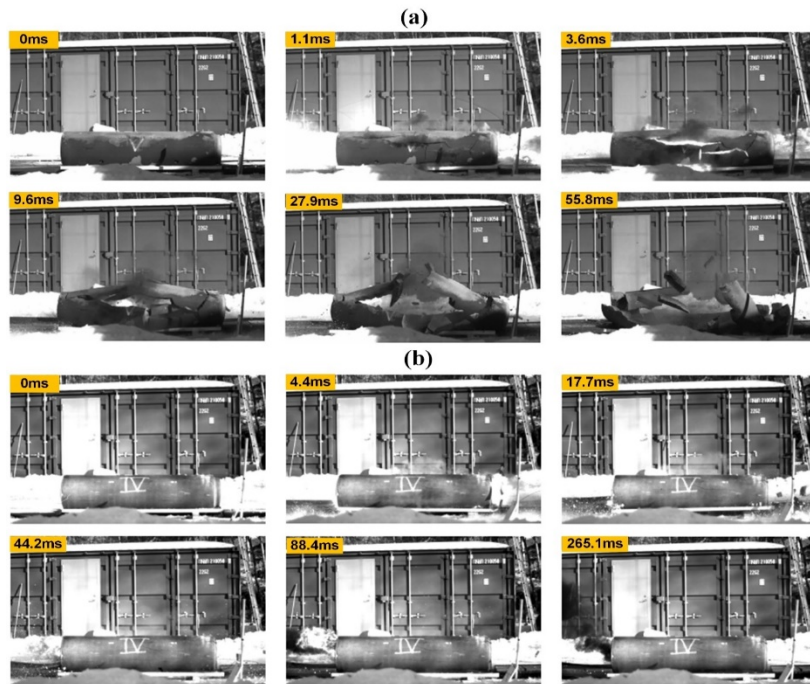
270 test conducted by Zhao, et al. (2016) investigated the dynamic response and damage of a segmental
271 lining tunnel under an internal high explosive explosion, as listed in **Table 8**. The test investigated
272 the response of tunnel lining under the eccentric detonation via the full-scale test. Apart from this
273 study, some other full-scale internal explosion experiments such as blasting induced vibration tests
274 inside tunnel (Ansell, 1999, Deng, et al., 2020) and internal explosion tests of ammunition storage
275 tunnel (Joachim, 1990, Zhou, 2011) were also reported in open literatures. Unlike the scarcity of
276 internal explosion scenarios, many full-scale external explosion experiments have been carried out
277 by surface pit blasting (Duan, et al., 2018, Jiang and Zhou, 2012, Shin, et al., 2011) and underground
278 cavern blasting (Liang, et al., 2012, Xia, et al., 2013, Zhao, et al., 2015) near tunnels to investigate
279 the dynamic response of tunnel against external explosion loads.

280 Compared to full-scale tests, more scaled-down tests were conducted over the past decades to
281 investigate the response of tunnels under different explosion scenarios. These scaled-down tests are
282 divided into two categories depending on whether the centrifuge device was utilized or not. On one
283 hand, many scaled-down tests have been conducted without using the centrifuge device. Blast loads
284 were generated by using high explosives (Chen, et al., 2014, 2015, Krone, 2018, Xie, et al., 2014,
285 Zhou, et al., 2020), ignited flammable materials (Groethe, et al., 2007, Meng, et al., 2020a, 2020b) or
286 blast simulating generators (Kiger, et al., 1989, Smith, et al., 1986, Tener, 1964) to investigate the
287 blast response of the scaled-down tunnels. Typical interaction processes between blast shock waves
288 and tunnel linings without and with reinforcement are shown in **Figure 7(a)** and **(b)**, respectively.
289 The scaled-down tunnels in **Figure 7** were placed on the ground and the influence of tunnel-
290 surroundings was not taken into consideration. The tunnel-surrounding interactions were not
291 considered in some other studies of scaled-down tunnel explosion tests either (Groethe, et al., 2007,
292 Kristiansen, 2019, Prochazka and Jandeková, 2020). The above scale-down tests under the normal
293 gravity are defective since the structural dead loads (i.e. gravity loads) are not scaled down (Townsend,
294 et al., 1987).

295 On the other hand, the centrifuge testing is a better way to solve the problem of gravity similarity.
296 A series of scaled-down centrifuge tests were conducted in the past to investigate the response of
297 tunnels under explosions (De, et al., 2013, 2016, 2017, Koneshwaran, et al., 2015a, Liu and Nezili,
298 2016, Soheyli, et al., 2016, Townsend, et al., 1987), some of which have been listed in **Table 8**.
299 However, these studies using the centrifuge mostly focused on investigating dynamic response of
300 tunnel with metal lining rather than RC lining to blast loads. In addition, it is worth pointing out that
301 the size of centrifuge model is small, which may not be able to predict the local damage and response

302 of tunnel structures. Meanwhile, complex tunnel structure involving structure joints, and secondary
 303 structures, etc., cannot be considered in the centrifuge test due to its small size.






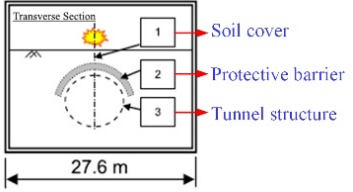
304 It is worth pointing out that most of the previous experimental tests were conducted by using high
 305 explosives. Very limited studies have investigated tunnel response under gas explosions. Meanwhile,
 306 the existing explosion experiments were mainly conducted in solid media. Experiment study on the
 307 response of tunnel in water has not been reported in open literature. In order to gain more
 308 comprehensive knowledge on the behaviour of tunnel, more tests including full-scale tests should be
 309 conducted under different explosion sources and in different buried media.

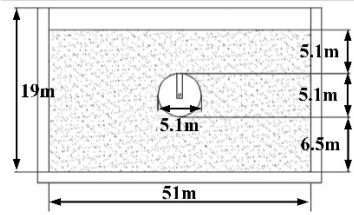
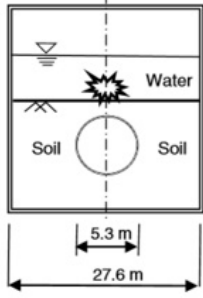


310 **Figure 7.** Damage process of (a) a plain concrete tunnel, and (b) a reinforced concrete (RC) tunnel under internally
 311 centric explosions with 100g C4 charge (Krone, 2018).
 312

313 **Table 8.** Experimental tests of tunnels subjected to explosion loads

Experimental test	Explosion type	Description of tunnel	Ref.	Experiment scene
Full-scale test	High explosive	5.5m inner diameter with the lining thickness of 0.4m and the axial length of 1.2m	(Zhao, et al., 2016)	

Scaled-down test	Without centrifuge	High explosive	2.9m inner span, 1.15m side wall height, the side wall lining thickness of 150mm, the floor lining thickness of 100mm, the axial length of 10m	(Chen, et al., 2014, Xie, et al., 2014)	
		BLEVE	A 78.5-m-long circular tunnel with a cross-sectional area of 3.74m ² .	(Groethe, et al., 2007)	
		High explosive	The tunnel length of 5 m, 0.5m and 1m inner diameters in two case. The lining thickness of 0.09m for both cases	(Prochazka and Jandeková, 2020)	
		High explosive	The inside span of 1.5m, the lining thickness of 120 mm in all sides	(Zhou, et al., 2020)	
		VCE (Methane-air)	The tunnel cross section of 1.6m*0.6m, the lining thickness of 0.1m, the longitudinal length of 20m, 9.5% methane concentration condition.	(Meng, et al., 2020a, Meng, et al., 2020b)	
Centrifuge test		High explosive	5.5 m outer diameter, 0.133 m lining thickness, 53m length of tunnel, copper as the material of tunnel structure (model scale = 1/70 prototype scale)	(De, et al., 2013, De, et al., 2016, Koneshwaran, et al., 2015a)	

High explosive	5.1m outer diameter and 8.25cm wall thickness, 25m length of tunnel, aluminum as the lining material (model scale = 1/50 prototype scale)	(Liu and Nezili, 2016)	
High explosive	5.5 m outer diameter of tunnel, 0.133 m lining thickness, 53m length of tunnel, copper as the material of tunnel structure (model scale = 1/70 prototype scale)	(De, et al., 2017)	

314
315

Table 9. Summary of current methods and instruments adopted for tunnel explosion tests

Test types	Test methods	Instruments	Advantages	Disadvantages
Full scale test	Field test	Explosive instruments	Directly measuring blast load, showing structural response and local damage	Costly, high risk, and time-consuming
Scaled-down tests without centrifuge	Field test	Explosive instruments	Reduced cost, directly measuring blast loading and showing structural response and local damage	Moderate risk, no scaled-down gravity load and material properties
	Laboratory test with explosive		Safe operation, no explosive required, cost-effectiveness	Not applicable for the internal explosion of tunnel
Scaled-down tests with centrifuge	Laboratory test without explosive	Blast simulating generator	Considering gravity similarity	Small model size, not considering complex tunnel structure, not predicting the local structural damage

316

4.1.3 Numerical methods

317

318

319

320

321

322

Due to the difficulty of experimental tests and the limits of theoretical methods, numerical method becomes a popular alternative for the analysis of tunnel structures subjected to explosion load. With the advances of computer power and computational mechanics in recent decades, numerous numerical tools have been developed (Hao, et al., 2016). Numerical simulations can not only predict blast load generation, wave transmission, wave-structure interaction and tunnel response, but also provide supplement data for the physical testing (Hao, et al., 2016). However, it should be noted that

323 a high-fidelity numerical model should be verified by reliable experimental data before it can be
 324 confidently used to predict the dynamic responses of tunnel structures under blast loads.

325 In the open literature, the commonly used numerical methods to investigate dynamic response of
 326 tunnel structures subjected to blast loads are based primarily on the traditional Lagrangian method
 327 (Buonsanti and Leonardi, 2013, Liang, et al., 2012, Mishra, et al., 2020, Mishra, et al., 2020), the
 328 coupled Eulerian-Lagrangian (CEL) method (Koneshwaran, 2014, Mandal, et al., 2020, Mussa, et al.,
 329 2017, Tiwari, et al., 2016), the boundary element method (BEM) (Shakeri, et al., 2020, Stamos and
 330 Beskos, 1995), the hybrid smoothed particle hydrodynamics (SPH)-finite element method (FEM)
 331 (Koneshwaran, et al., 2013, 2015b, 2015c, Wang, et al., 2005), the discrete element method (DEM)
 332 (Deng, et al., 2014, Xia, et al., 2013), the hybrid FEM-DEM (Mitelman and Elmo, 2014, 2016), and
 333 the coupled Godunov-variational difference method (VDM) (Feldgun, et al., 2008, 2013a, 2013b,
 334 2014), etc. Their advantages and disadvantages are summarized in **Table 10**. These numerical
 335 methods have embedded in some numerical software, such as LS-DYNA, AUTODYNA, ABAQUS,
 336 and UEDC, etc, whose characteristics, advantages and disadvantages are summarized in **Table 11**.

337 **Table 10.** Summary of numerical methods for dynamic response of tunnel subjected to blast loads

Category	Advantage	Disadvantage
Lagrangian method	Fast calculation; Suited to treat inhomogeneous, anisotropic materials with nonlinear behaviour	Prone to experience severe mesh distortion and computational overflow; Requiring artificial boundary in infinite or semi-infinite models such as non-reflection boundary
CEL	Considering the interaction between blast wave and structure; Effectively reducing mesh distortion	Strongly relying on the element size; Computationally time-consuming; Blurry material interface in Eulerian element
BEM	Not requiring artificial boundaries; Reducing calculated dimensionality in infinite or semi-infinite domains compared to FEM	Not suited to inhomogeneous, anisotropic materials (e.g., concrete, rock) with nonlinear behavior
SPH-FEM	Not requiring mesh for SPH; Suited to extreme distortion situation; Not requiring material track	Computationally time-consuming
DEM	Allowing finite detachments and rotations of discrete blocks of tunnel structure; Enable to model fragment of tunnel under blast loads	Computationally time-consuming; Not realistically predicting the crack initiation and propagation of tunnel owing to the pre-defined discretization models
Hybrid FEM-DEM	Allowing realistic simulation of brittle fracture-driven processes of tunnel and a full consideration of failure kinematics	Computationally time-consuming due to re-meshing procedures
Coupled Godunov-VDM	Addressing large deformations and buckling of the tunnel lining	Not suited to model fragment of tunnel lining

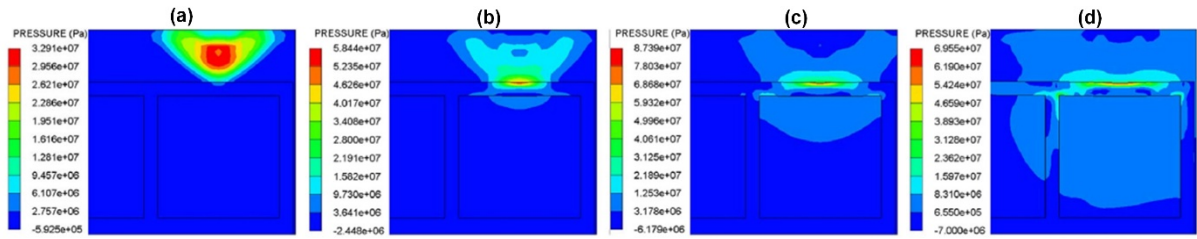
339 **Table 11.** Summary of commonly used software packages for dynamic response of tunnel subjected to blast loads

Software	Characteristics	Function	Advantage	Disadvantage
ANSYS/ LS-DYNA	Explicit algorithm for explosion analysis, based on finite element method	Simulating explosive detonation and its interaction with tunnel; Modelling the nonlinear tunnel response	Abundant material models for concrete and reinforcement; Multiple ways to simulate blast wave propagations	Less geotechnical material model; computational costly with refined mesh
ANSYS/ AUTODYN	Explicit algorithm for explosion analysis, based on finite difference method	Simulating explosive detonation with afterburning effect; Modelling blast wave interaction with tunnel; Modelling the nonlinear tunnel response	Allowing modelling detonation with high grid resolution without increasing computational cost; Being good at multi-physics coupling problem	Less geotechnical material model
ABAQUS	Explicit algorithm for explosion analysis, based on finite element method	Simulating blast wave interaction with tunnel by CEL method; Modelling the nonlinear tunnel response	Multiple available soil and rock material models; Stable calculating ability	Less concrete model; computational costly with refined mesh
UEDC	Based on block discrete element method	Modelling discontinuous block media such as joint rock	Modelling the energy dissipation during the fracture process and the kinetic energy of each discrete block	Computational costly; Not simulating real crack process

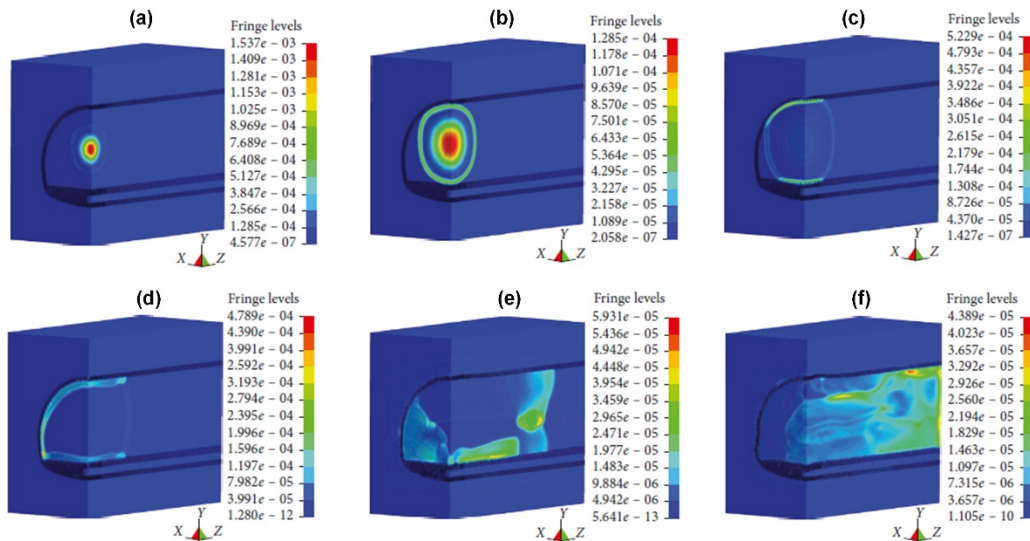
340

341 Most of these numerical methods can intuitively show the propagation of blast wave and its
342 interaction with lining structures. For instance, Yang, et al. (2018) used the CEL method to investigate
343 the whole process of shock wave propagation and its interaction with a multi-cell rectangular tunnel
344 in an external explosion scenario, as shown in **Figure 8**. Meanwhile, Li, et al. (2018) investigated the
345 detailed propagation process of shock wave inside the tunnel for an internal explosion by the CEL
346 method, as shown in **Figure 9**. These numerical methods are mostly conducted to investigate dynamic
347 response of tunnel subjected to high explosive explosions, in which the explosion loads are obtained
348 by using conventional weapons effects program (CONWEP) and computational fluid dynamics (CFD)
349 method, etc. It should be noted that the above-mentioned high-explosive-based numerical methods
350 may not give accurate prediction of explosion loads from gas explosions, especially when the standoff
351 distance is short (Li and Hao, 2020, 2021). Two studies (Molenaar, et al., 2009, Vervuurt, et al., 2007)
352 using multiple energy method and one study (Wang, et al., 2021) based on simplified overpressure-
353 time history of gas deflagration numerically investigated the dynamic response of tunnel subjected to
354 internal gas explosions. The multiple energy method and the simplified method were developed to

355 predict explosion load from gas explosion at ground surface or in free air, ignoring the multiple
 356 interactions between blast waves and lining. In addition, in the case of gas explosion, the damage of
 357 tunnel could be caused by the coupling effect of explosion and fire if the material involved is
 358 flammable. In open literature, only two studies (Buonsanti and Leonardi, 2013, Colombo, et al., 2015)
 359 investigated the dynamic response of tunnels against the combination of pre-explosion fire and
 360 followed explosion. No study in open literature has investigated the influence of pre-explosion
 361 followed by fire on the dynamic response of tunnel.



362
 363 **Figure 8.** Propagation of surface explosion pressure waves at (a) 2ms, (b) 3ms, (c) 4ms, and (d) 5ms, respectively
 364 (Yang, et al., 2018).



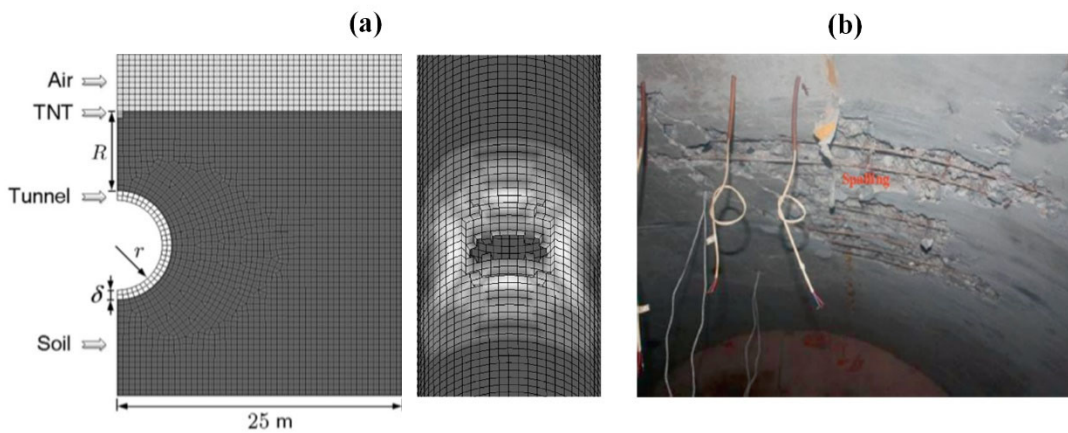
365
 366 **Figure 9.** Propagation of blast shock wave inside a tunnel at (a) 0.5ms, (b) 0.98ms, (c) 1.3ms, (d) 2.2ms, (e) 7ms, and
 367 (f) 12ms. The units are 10^2 GPa (Li, et al., 2018).

368 4.2 Forms of damage and response of tunnels under explosions

369 In addition to the above-reviewed analysis methods, the forms of damage and response of tunnels
 370 under blast loads are reviewed and classified in this section. The damage and response forms can be
 371 mainly classified as crushing and spalling of tunnel linings, cracks of tunnel linings, deformation and
 372 collapse of tunnel lining, bending and tensile failures of reinforcements, and damage of tunnel
 373 surroundings, which are reviewed in details in this section.

374 **4.2.1 Crushing and spalling of tunnel linings**

375 The tunnel lining may suffer both crushing and spalling damages under external explosions, while
376 the tunnel is prone to experience crushing subjected to internal explosions. Under the external
377 explosion load, the crushing usually appears on the outer surface of the tunnel lining, where the
378 superposition of the incident wave and reflected wave at the interface of lining and surroundings
379 intensifies the compressive stress waves. The spalling damage occurs on the inner surface of the lining
380 under external explosion, which is due to the tensile action of stress wave in the tunnel lining. The
381 typical crushing and spalling damages of tunnel lining under external blast loads is shown in **Figure**
382 **10(a)** and (b). Under internal explosions, the crushing can occur at both the inner surface and the outer
383 surface of lining. Due to the intensification of reflected compressive waves on the inner surface of
384 lining, the crushing of inner surface first occurs and continuously propagates outwards in the tunnel.
385 Meanwhile, when the transmitted stress waves reach the interface of lining-surroundings, the
386 compressive stress waves reflect again due to the difference of wave impedance between
387 surroundings and the lining. The reflected waves further intensify the stress waves, which might lead
388 to the crushing at the outer surface of tunnel lining. The combined effect of the inner and the outer
389 crushing of tunnel lining may breach the tunnel lining.

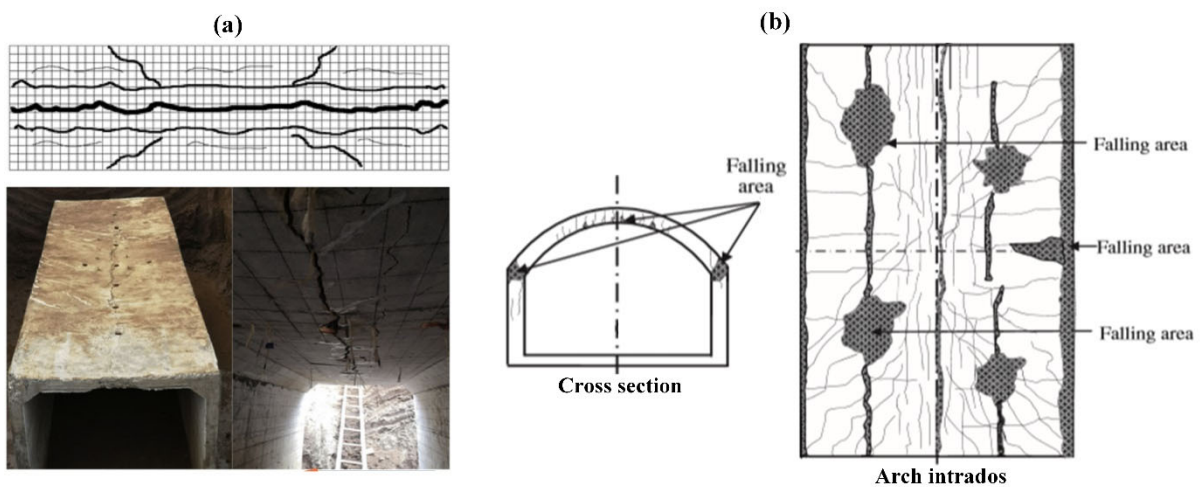


390
391 **Figure 10.** The crushing and spalling damage of tunnel lining under external blast loading. (a) the crushing damage of
392 tunnel lining (Mobaraki and Vaghefi, 2016), and (b) the spalling damage of tunnel lining (Chen, et al., 2015).

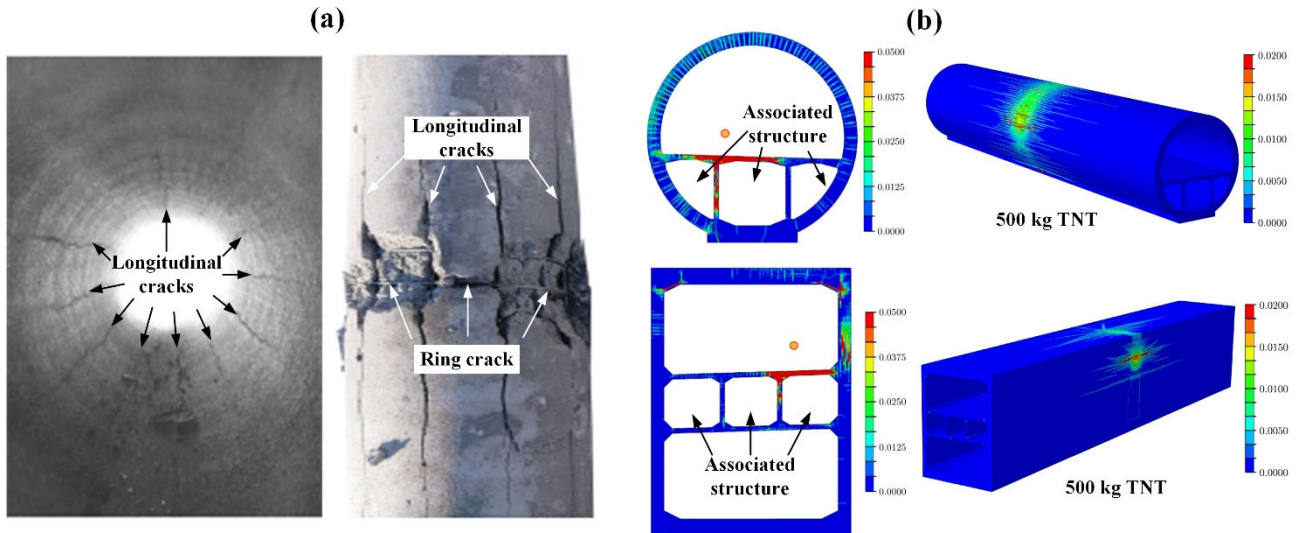
393 **4.2.2 Cracks of tunnel linings**

394 The cracks of tunnel linings usually appear outside the spalling and crushing zones or collapse
395 zones (Chen, et al., 2014, Li, et al., 2018, Yang, et al., 2019), or on the tunnel lining near detonation
396 under low-intensity blast loading (Koneshwaran, et al., 2015b, Krone, 2018, Zhao, et al., 2016), or
397 on the whole section of tunnel lining along the longitudinal direction (Stolz and Ruiz-Ripoll, 2015,
398 Zhou, et al., 2020). Under external explosions, the presence of these cracks are mainly attributed to
399 the overall bending deformation of tunnel lining and the reflected tensile damage. As reported by

400 Zhou, et al. (2020), due to the downward bending deformation of the tunnel roof, three longitudinal
 401 cracks along the mid-span of whole roof were observed in the external surface explosion experiment,
 402 as shown in **Figure 11(a)**. In addition to the crack damage induced by the bending deformation, Chen,
 403 et al. (2014) observed that due to the reflected tensile damage, oblique cracks and ring cracks around
 404 spalling areas on the inner surface of an arch tunnel lining were formed after a series of external
 405 explosions (see **Figure 11(b)**). Under the internal explosion, the cracks of tunnel lining are usually
 406 formed due to the radial expansion deformation of tunnel lining with the increased hoop tensile stress
 407 of tunnel lining. As reported by Krone (2018), due to the radial expansion of tunnel lining under
 408 internal explosion, the ring cracks appeared on the tunnel lining near detonation, and the longitudinal
 409 cracks on tunnel lining were observed outside the ring cracks, as shown in **Figure 12(a)**. In the
 410 numerical study, Kristoffersen, et al. (2019) also observed the crack damage on the circular and
 411 rectangular submerged float tunnels under an internal eccentric explosion with 500 kg TNT charge,
 412 as shown in **Figure 12(b)**. In addition, the cracking behaviours of tunnel with segmental linings under
 413 internal explosion were experimentally investigated by Zhao, et al. (2016). They found that the joints
 414 between segments were more prone to be cracked due to stress concentration at the connection of
 415 joints.



416
 417 **Figure 11.** The crack damage of linings with (a) rectangular tunnel subjected to external explosion load (Zhou, et al.,
 418 2020), and (b) arch tunnel subjected to external explosion load (Chen, et al., 2014).



419

420

421

Figure 12. The crack damages of (a) a circular tunnel lining under an internal centric explosion (Krone, 2018), and (b) circular and rectangular submerged float tunnels under an internal eccentric explosion (Kristoffersen, et al., 2019).

422

423

424

425

426

427

428

It is worth noting that associated structures of two tunnels in **Figure 12(b)** were also seriously damaged by the internal explosion. Due to the lack of surrounding support, the associated structures of tunnel, e.g. escape and smoke passages are more vulnerable to blast loads than main structure (i.e. lining) of tunnel. The damage of associated structures could significantly interrupt the transportation functionality of road tunnels, and even induce severe casualties. However, very limited studies have investigated the response of associated structures under blast loads, which is deemed necessary for further study.

429

4.2.3 Deformation and collapse of tunnel linings

430

431

432

433

434

435

436

437

438

439

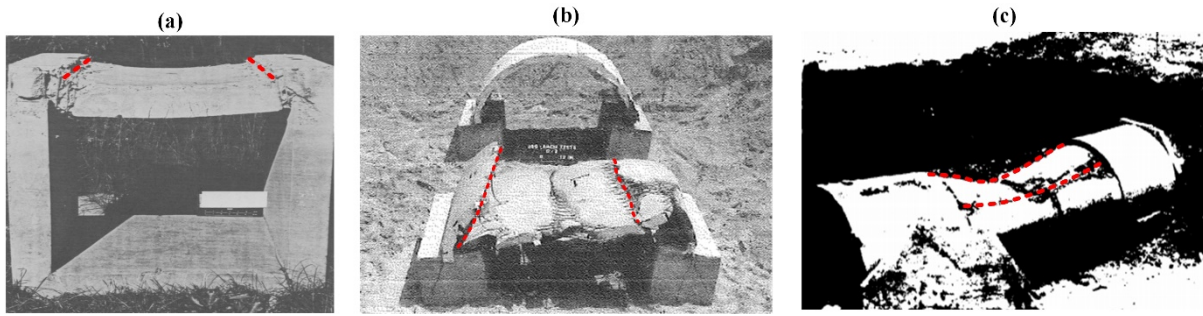
440

441

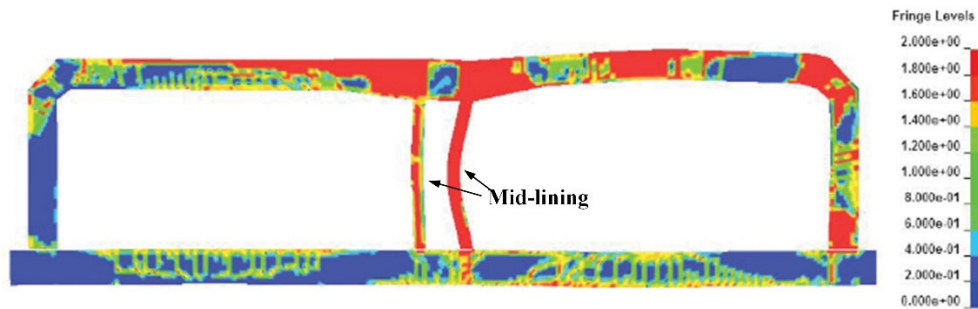
442

With the presence of cracks, tunnel linings might experience large deformation or collapse. Under external explosion, the tunnel lining directly facing blast loadings is usually deformed towards the inner of tunnel (Slawson, 1984). When tunnels suffer intensive external blast loads, the collapse of tunnel lining could occur. It was reported by Kiger, et al. (1989) and Smith, et al. (1986) that the tunnel-like arches buried in soil collapsed under intensive surface explosion. **Figure 13(a)-(c)** show the deformation and collapse after removing the buried soil. When two penetrating cracks along the haunches or roof corners of tunnel lining at both sides are formed, the tunnel lining deforms or collapses. Moreover, for segmental lining, the deformation patterns of radial dislocations between adjacent segments and longitudinal dislocations between adjacent lining rings might occur under external explosions (Koneshwaran, 2014, 2015b). Under internal explosions, the tunnel linings normally expand radially outward if the intensive incident pressure can overcome the blocking action of tunnel surroundings (Han, et al., 2016, Li, et al., 2018). Other types of deformation patterns could occur under eccentric internal explosion. For instance, when internal explosion occurs near bottom

443 lining, Zhao, et al. (2016) observed an elliptical deformation of a circular tunnel lining, i.e., the
444 expansion of the upper and lower tunnel lining and the inward deformation of two side linings. When
445 a multi-cell tunnel is subjected to an internal explosion, the mid-lining wall might experience
446 deformation and collapse due to the lack of surrounding support, as shown in **Figure 14**. Currently,
447 very limited studies have investigated the damage of mid-lining of multi-cell tunnel under internal
448 explosion.



449
450 **Figure 13.** The collapse of tunnel linings under external explosion. (a) permanent deformation of tunnel-like box roof
451 (Slawson, 1984), (b) collapse of tunnel-like arch structure (Kiger, et al., 1989), and (c) vault collapse of tunnel-like arch
452 structure (Smith, et al., 1986).



453
454 **Figure 14.** The deformation and damage of a rectangular tunnel lining under internal explosion (Molenaar, et al., 2009).

455 4.2.4 Bending and tensile failure of reinforcement

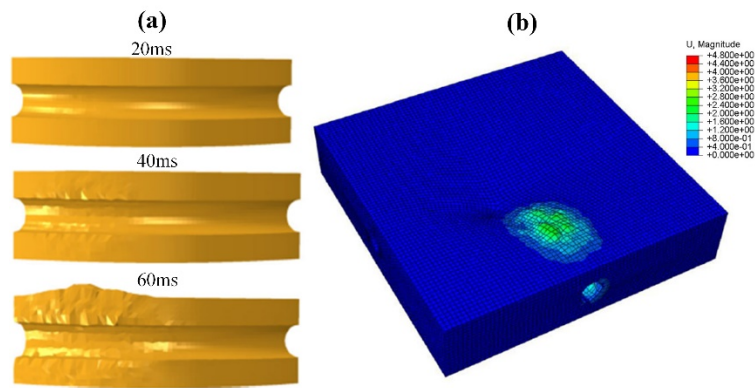
456 The bending and tensile failure of reinforcement in tunnel lining was often observed under
457 external explosion. Chen, et al. (2015) reported that the arch roof of a tunnel-like structure
458 experienced severe bending damage of the longitudinal and hoop reinforcements under a series of
459 external explosions, especially at the conjunction of roof and sidewall, as shown in **Figure 15(a)**.
460 Meanwhile, with the presence of longitudinal structural cracks on tunnel lining, hoop steel bars across
461 the longitudinal cracks were stretched to fracture, as shown in **Figure 15(b)**. It was also reported by
462 Smith, et al. (1986) that under surface explosions the lining structure experienced catastrophic
463 collapse, along with bending and tensile failures of reinforcement. However, there is no report on
464 bending and tensile failure of lining reinforcement when subjected to internal explosion.



465
466 **Figure 15.** The bending and tensile failures of reinforcement (Chen, et al., 2015). (a) bending failure, and (b) tensile
467 failure.

468 4.2.5 Deformation and damage of tunnel surroundings

469 The deformations of tunnel surroundings involve the deformation around tunnel and the ground
470 heave. Under internal blast loads, the deformation around a shallow buried tunnel first occurs and
471 then the ground deformation above tunnel is possible with the propagation of blast-induced stress
472 waves. As reported by Tiwari, et al. (2018), an obvious ground heave above a circular curved tunnel
473 was simulated under an internal explosion, as shown in **Figure 16**. The large ground deformation
474 might potentially damage surface structures (e.g. the multi-storey buildings) near the tunnel.
475 Therefore, the stability of buildings near the tunnel subjected to explosion loads need be evaluated.



476
477 **Figure 16.** The ground heave above a curved tunnel under internal blast loading (Tiwari, et al., 2018). (a) the
478 deformation process of tunnel surroundings, and (b) the aerial view of the ground heave (The unit of U is m).

479 In addition to the deformation, tunnel surroundings might be subjected to the blast induced
480 damage and collapse under high-intensity explosion loadings. In some existing studies (Deng, et al.,
481 2014, Hao and Wu, 2001, Mitelman and Elmo, 2014, 2016, Wu and Hao, 2006), the damage and
482 collapse of the surroundings of tunnel or tunnel-like structure without the lining supports were
483 investigated under internal and external explosions. For example, Hao and Wu (2001) numerically

484 investigated the damage zones of surroundings of a tunnel-like rock chamber under the internal blast
485 loadings with different loading densities. As expected, more damage was generated in the rock mass
486 with the increasing loading density. Mitelman and Elmo (2014) investigated the collapses of
487 surroundings for unlined tunnels under external explosions. It was observed that the main collapse
488 zones occurred above the tunnel roof, which had closer distance to the external explosion centre than
489 other tunnel parts. Although the surroundings of road tunnels are usually supported by the lining
490 structure, very limited studies on the collapse of tunnel surroundings with the support of lining under
491 internal and external explosions have been conducted.

492 **4.3 Influence factors of tunnel response subjected explosion loads**

493 Dynamic response and damage levels of tunnels subjected to blast loads are affected by various
494 factors. In this section, the key factors influencing the tunnel response and damage are presented.

495 **4.3.1 Equivalent charge weight**

496 The equivalent charge weight is one of decisive factors affecting the peak pressure acting on
497 tunnel structures and the damage of tunnel structures. In the previous studies, the effect of charge
498 weight on the tunnel response was investigated with respect to various parameters including
499 displacement (Dhamne, et al., 2018, Koneshwaran, et al., 2015c, Yang, et al., 2018), pressure (Choi,
500 et al., 2006, Han, et al., 2016, Yang, et al., 2010), stress (Parviz, et al., 2017, Prasanna and
501 Boominathan, 2014), strain (Kristoffersen, et al., 2019, Liu, 2012), acceleration (Soheyli, et al., 2016)
502 and velocity (Lu, et al., 2016, Mussa, et al., 2018). It is noted that the equivalent conversion from gas
503 explosive to high explosive might not give accurate predictions of the overpressure from gas
504 explosions, especially for the overpressure of near-field explosions, which might cause the inaccurate
505 predictions of the tunnel response and damage.

506 **4.3.2 Standoff distance**

507 The standoff distance between tunnel structure and explosive as a critical factor has been widely
508 investigated. Under the internal blast loading, standoff distance can be varied by changing the size of
509 tunnel cross section with the determined explosive location (Choi, et al., 2006). By increasing the
510 size of tunnel cross section, the loading density defined as the ratio of explosive weight to internal
511 space decreases given the same explosive weight, which results in the decreased explosion load acting
512 on the tunnel structures. Under external blast loading, the standoff distance varies by changing the
513 location of tunnel with the determined explosive location (Mobaraki and Vaghefi, 2015, Yang, et al.,
514 2018, Yang, et al., 2010), or changing the location of explosive with the determined tunnel location
515 (Yang, et al., 2019, Yankelevsky, et al., 2012) for single tunnel, and changing the spacing between

516 tunnels for neighbouring tunnels (Mo, et al., 2013, Prasanna and Boominathan, 2014). With the
517 increased standoff distance between the tunnel and the charge, the intensity of external blast pressure
518 acting on the tunnel structures reduces and hence structural damage decreases.

519 **4.3.3 Burial depth of tunnel**

520 Varying burial depth of tunnel results in various confinement levels to tunnel structures. For the
521 relatively shallow buried tunnel, increasing confinement levels with the increased burial depth of
522 tunnel suppress the deformation and vibration response of tunnel subjected to explosions, which is
523 beneficial to reduce the damage of tunnel. As reported by Yu, et al. (2015), with the burial depth
524 increased from 6m to 12m, the effective plastic strain at the vault of the circular tunnel decreased
525 under the internal explosion. However, for the relatively deep buried tunnel, the increase of
526 confinement levels by increasing the burial depth usually results in more strain energy accumulated
527 around the tunnel due to the increased in-situ stress. The release of higher strain energy with blast
528 load as a trigger is adverse to the stability of tunnel. As reported by Li, et al. (2018), the damage of
529 tunnel with the burial depth over 500m was more severe than that at the burial depth of 500m. It is
530 noted that no existing study has provided the specific depth ranges for shallow and deep buried tunnels.
531 The depth ranges of shallow and deep buried tunnels might vary with different geological conditions.
532 The influence of burial depth with respect to different geological conditions on the dynamic response
533 of tunnel subjected to blast loads should be investigated and the depth ranges for shallow and deep
534 tunnels can be specified in the future study.

535 **4.3.4 Charge position**

536 Charge position could be changed in the same cross-section plane of tunnel or along the
537 longitudinal direction of tunnel. Tiwari, et al. (2015) investigated the effect of variation of charge
538 position along the longitudinal direction of a curved tunnel on the dynamic response of tunnel under
539 internal explosion. The results indicated that when the explosive was placed in the longitudinal centre
540 of tunnel as compared to that at the quarter of tunnel along the longitudinal direction, larger
541 deformation of lining and surroundings was observed due to longer venting time of explosive cloud.
542 In the same cross-section plane of tunnel, the charge position could vary both inside (Colombo, et al.,
543 2016, Feldgun, et al., 2014, Yu, et al., 2015) and outside (Koneshwaran, et al., 2015d) tunnel. For
544 instance, for the charge inside tunnel, a study conducted by Feldgun, et al. (2014) investigated the
545 pressure distributions on the walls of a rectangular tunnel under centric explosion and eccentric
546 explosion near floor. The results indicated that the maximum peak pressure on tunnel lining under
547 the eccentric explosion was higher than that under the centric explosion. Overall, the tunnel was safer
548 under the centric explosion. In actual operating road tunnel, explosions could happen at different

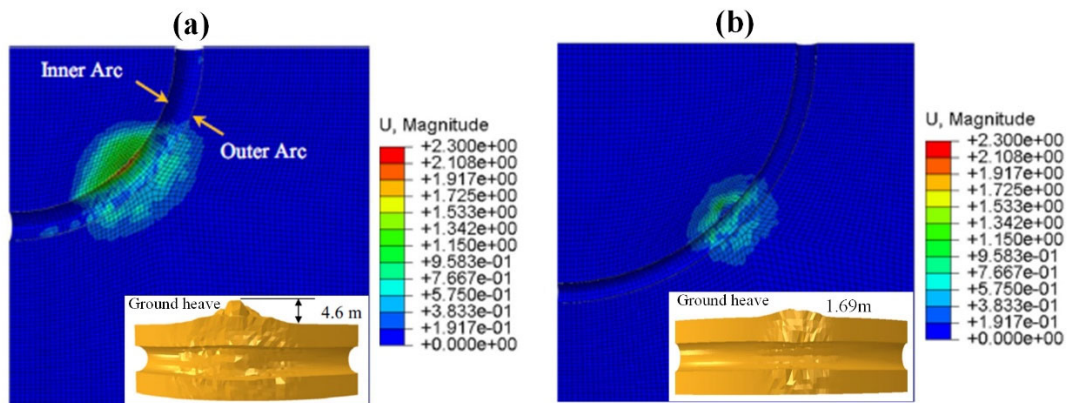
549 locations on the tunnel floor. However, no study has been conducted on the influence of internal
550 explosions at different locations of tunnel floor on dynamic response of tunnel. With regard to the
551 charge position outside the tunnel in the same cross-section plane, Koneshwaran, et al. (2015d)
552 investigated the influence of varying charge position on the ground surface, where two same charges
553 were located on the ground directly and obliquely over the tunnel with the same standoff distance.
554 The results showed that the tunnel directly below the charge was more vulnerable to the surface
555 explosion than the tunnel obliquely below the charge. It should be noted that the tunnels with
556 rectangular or arched cross sectional shapes subjected to external explosions at various locations and
557 standoff distances have not been studied yet.

558 **4.3.5 Shapes of tunnel**

559 Tunnel has different shapes in the cross section and the longitudinal directions. Varying the shape
560 of cross section influences many other factors, such as the interaction area between surroundings-
561 structure, the cross sectional curvature, the cross sectional dimension, the standoff distance and the
562 tunnel aspect ratio, which may affect the load-carrying capacity of tunnel. Mobaraki and Vaghefi
563 (2015) found that as compared to the tunnels with circular, box and arched cross sections, the semi-
564 ellipse tunnel had the least damage under the same external explosion due to its maximum contact
565 zone between the soil and tunnel in the study, thereby increasing the stability of the semi-ellipse
566 tunnel. However, the contribution of other influencing factors to the stability of the tunnel, especially
567 the difference in cross-sectional dimensions and aspect ratios, was not considered in this study. When
568 the standoff distance from the centre of external explosion to tunnel wall is kept the same, the smaller
569 cross section dimension is usually more beneficial to the blast resistance of tunnel (Wu, et al., 2011).
570 If the cross-sectional dimensions of the tunnel are similar, the greater the aspect ratio (the ratio of
571 height to span) of the tunnel is, the more sensitive the dynamic response of tunnel to blast loads would
572 be (Dhamne, et al., 2018, Wu, et al., 2011). When the cross sectional dimensions and aspect ratios of
573 tunnels are similar and the standoff distance from explosion centre to the tunnel wall is kept the same,
574 the circular tunnels have better resistance against external explosions than others (Mandal, et al.,
575 2020). It is because the curvature of circular tunnel results in less reflected pressure on the tunnel
576 structures (Gebben and Döge, 2010). Under internal explosion, some studies (Goel, et al., 2020,
577 Prasanna and Boominathan, 2020) concluded the curvature of circular tunnel could cause more even
578 distribution of blast load on the tunnel structure than box tunnel with similar height and span, thereby
579 having a better blast resistance. However, a numerical study conducted by Yu, et al. (2015)_found
580 that the maximum plastic strains on the lining of the circular tunnel subjected to an internal centric
581 explosion were higher than those of the square-shaped tunnel with similar cross sectional dimension.

582 Further work should be conducted to reveal the effects of different shapes of cross section with similar
 583 cross-sectional dimension on the response of tunnel subjected to internal explosions.

584 Very limited studies have been conducted with respect to the influence of the longitudinal shape
 585 of tunnel on the dynamic response of tunnel to blast loads. One study conducted by Tiwari, et al.
 586 (2018)_investigated the influence of radii of tunnel curvature in the longitudinal direction on the
 587 response of tunnel. Two curved tunnels with the curvature radii of 30m and 70m were subjected to
 588 the same internal explosion. The soil around tunnel and the ground directly above the tunnel with the
 589 tunnel curvature radius of 30m experienced larger deformation than those with the curvature radius
 590 of 70m (see **Figure 17**). It is because the smaller curvature radius (30m) is apt to contain blast wave
 591 inside tunnel and induce more reflections of blast wave inside tunnel. Besides the curved tunnel, the
 592 sloped tunnel has been constructed whilst the influence of slope of the tunnel on the blast response of
 593 tunnel has not been investigated.



594
 595 **Figure 17.** The deformation around tunnel and the ground heave above the tunnel with the curvature radius of (a) 30m,
 596 and (b) 70m (Unit of U is m) (Tiwari, et al., 2018).

597 4.3.6 Physical and mechanical properties of lining and surroundings

598 The existing studies regarding the influence of lining material properties on the response of tunnel
 599 focus on the influence of the lining stiffness (Han, 2014), the lining strength (Khan, et al., 2016), the
 600 lining damping (Han, 2014), the lining brittleness (Liu, 2012), the lining thickness (Mussa, et al.,
 601 2017, Prasanna and Boominathan, 2020, Tiwari, et al., 2017), the type of lining material (Chaudhary,
 602 et al., 2018, Colombo, et al., 2015, Parviz, et al., 2017), and joint types for segmental lining and the
 603 number of segments (Koneshwaran, 2014). **Table 12** summarizes their influences on the dynamic
 604 response of tunnel subjected to blast loads.

605 **Table 12.** The influence of lining properties on the dynamic response of tunnel subjected to blast loads

Factor	Effectiveness on the blast resistance of tunnel
--------	---

Increase lining stiffness	Significantly enhance the resistance of lining to bending and deformation
Increase lining strength	Enhance the anti-damage ability of tunnel lining
Increase lining damping	Decrease the damage levels of tunnel due to stronger ability to absorb explosion energy
Decrease lining brittleness	Improve the vulnerability of lining against rupture
Increase lining thickness	Decrease the damage of tunnel due to the increased moment of inertia
High-performance lining material	Decrease damage levels of tunnel due to high strength, high stiffness and high energy absorbing ability of material
Joint type for segmental lining (Koneshwaran, 2014)	(Convex-concave joint compared with flat joint) Reduce the drifting response of tunnel at joint due to the mechanical interlocking; (Convex-convex joint compared with flat joint) Reduce the crack levels at joint due to less friction areas between segments and more dependence on the joint bolt
Increase the number of segments	Reduce the cracks of lining under small blast loads due to the increased flexibility

606 The effects of tunnel surroundings including rock mass and soil on the dynamic response of tunnel
607 under explosions have been comprehensively investigated by considering the water contents of
608 surrounding medium (Al-Damluji, et al., 2010, Koneshwaran, et al., 2015d, Osinov, et al., 2019),
609 strength (Tiwari, et al., 2016, 2017), stiffness (Liu, 2009, Verma, et al., 2017, Yang, et al., 2010),
610 density of surrounding medium (Higgins, et al., 2013, Parviz, et al., 2017, Stolz and Ruiz-Ripoll,
611 2015), damping ratio (Dang, et al., 2018, Gui and Chien, 2006), wave impedance (Chen, et al., 2013a,
612 2013b), joint performance in tunnel surroundings (Deng, et al., 2014), and lateral pressure coefficients
613 (Li, et al., 2018). **Table 13** summarizes their influences on the dynamic response of tunnel under
614 explosions. It is found that very limited study has investigated the influence of the interface properties
615 between lining and surroundings on the dynamic response of tunnel under explosions.

616 **Table 13.** The influence of surroundings properties on the dynamic response of tunnel subjected to blast loads

Factor	Effectiveness on the blast resistance of tunnel
Increase water content	Decrease the damage of tunnel under low blast pressure due to the reduction of the blast load acting on soil skeleton with the water sharing; Increase the damage of tunnel under intensive blast loads due to the water weakening on soil skeleton and the instant increase of undrained pore pressure
Increase stiffness of surroundings	Decrease the blast damage due to the increase of resistance of surroundings to deformation

Increase strength of surroundings	Reduce the damage of tunnel surroundings while not significantly reduce the response of tunnel lining
Increase density of surroundings	Reduce the damage of tunnel lining under internal explosion due to its enhanced support; Increase the damage of tunnel lining under external explosion due to more blast wave transferred to the tunnel
Higher damping of surrounding	Absorb more blast energy and thus reduce the damage of tunnel under external explosion
Lower wave impedance	Reduce the damage of tunnel under external explosion due to more attenuation of blast wave
Joint performance of tunnel surroundings	(Small joint dip angle, large joint stiffness and small joint spacing) Enhance the resistance of tunnel against blast loading
Increase lateral pressure coefficient	Increase strain energy stored around the tunnel and thus damage tunnel more severely with its release under blast loads

617 5. Assessment of tunnel damage under explosion

618 Damage assessment of tunnel under explosions is critical for the design of tunnel structure and
619 subsequent retrofitting. By far, there are many available criteria for assessing and predicting the
620 consequences of tunnel damage, i.e., the deflection or deflection-span ratio, peak particle velocity
621 (PPV), crack grades, moment-force interaction diagram, pressure-impulse diagram, diagram of
622 charge weight versus standoff distance, and the empirical equation of spall and breach. Depending
623 on the spans of tunnels, these methods are readily used to evaluate the overall failure as well as the
624 local damage of tunnel structures. The specific details of the methods are reviewed below.

625 5.1 Based on deflection or deflection-span ratio

626 The damage assessment based on deflection or deflection-span ratio is achieved by simplifying
627 the tunnel structure into an equivalent elastic-perfect-plastic single degree of freedom (SDOF) model
628 (Mussa, et al., 2017). Since the SDOF approach is based on the assumption that the first mode of the
629 structure is the dominant response mode, various damage levels of tunnel structures corresponding to
630 the maximum mid-span deflection of tunnel wall were suggested (Mussa, et al., 2018). **Table 14** gives
631 the damage index related to the deflection, the deflection-span ratio, and the ratio of deflection to
632 half-span. These damage criteria were proposed based on the assumption of global ductile response.
633 Therefore, it is not applicable to apply the criteria for the cases of shear response and localized
634 concrete crushing and spalling response (Hao, 2015). In other words, the damage criterion is suitable
635 for the damage assessment of tunnel structures where the flexural mode is dominant.

Table 14. The damage criteria related to deflection for tunnel structure under blast loading

Ref.	Criterion index	Damage levels/damage index			
		Slight damage	Moderate damage	Severe damage	Collapse
(Mussa, et al., 2017)	Deflection	<20mm	20-40mm	40-80mm	>80mm
(Yang, et al., 2019)	Deflection-span ratio	<1/200	1/200-1/100	1/100-1/50	>1/50
(Ma, et al., 2008, 2010)	Deflection to half-span ratio	2.5%	6.0%	12.5%	-

637 5.2 Based on peak particle velocity

638 The damage assessment of tunnel based on peak particle velocity (PPV) could be divided into
639 two categories. The first category only gives a damage threshold of PPV, which is usually determined
640 by establishing empirical relationships between effective stress/strain and PPV (Jiang and Zhou, 2012,
641 Liang, et al., 2012, Liu, et al., 2019, Mobaraki and Vaghefi, 2015), in which the PPV is proportional
642 to the energy of blast shock wave and structural stress/strain. When the effective stress or strain
643 reaches allowable maximum limit of tunnel structure material, e.g, the maximum strength or failure
644 strain of lining material, the corresponding PPV threshold is obtained by using the established
645 empirical equation. The second category provides the PPV thresholds of different damage levels
646 based on experimental or numerical observations. Some studies (Hendron, 1978, Li and Huang, 1994)
647 suggested the PPV thresholds for different damage levels of the unlined tunnel. A comprehensive
648 study of unlined tunnel damage was the US Army's Underground Explosion Tests (UET), as reported
649 in Hendron (1978). In the study, the tunnel damage was classified into four damage zones along the
650 longitudinal direction of tunnel, i.e. the intermittent failure zone with the PPV of 0.9 m/s-1.8 m/s, the
651 local failure zone with the maximum PPV limit of 4 m/s, the general failure with the maximum PPV
652 limit of 12 m/s, and the tight closure zone. However, the road tunnels are usually supported by lining.
653 Only limited studies gave the PPV thresholds for different damage levels of the lined tunnel. Dowding
654 (1984) reported that the damage levels of lined tunnel could be divided into four categories, i.e.,
655 cracking of lining with the PPV limit of 1m/s, displacement of cracks with the PPV limit of 1.3 m/s,
656 local failure with the PPV limit of 7.4 m/s, and complete failure with the PPV limit of 40 m/s. In
657 another study, Mussa, et al. (2018) determined the PPV thresholds for different damage levels of the
658 tunnel lining with three different thicknesses by matching damage results to those based on the
659 criterion of deflection-span ratio. It is noted that the damage criterion based on PPV is site-dependent,
660 i.e., related to the specific properties of tunnel lining and surrounding materials.

661 It has been well known that the damage status of tunnel structures is not only related to the PPV
 662 but also the frequency of blast wave. The blast damage levels of tunnel could vary significantly under
 663 different main frequency bands of blast wave with the same PPV and tunnel condition. In other words,
 664 the tunnel response and damage depend not only on the blast wave amplitude, i.e., PPV, but also on
 665 its frequency contents. However, no study has considered the influence of blast wave frequency on
 666 the PPV-based damage criteria for tunnel structures.

667 **5.3 Based on crack grades**

668 The crack-grade-based damage assessment method is usually established by observing the cracks
 669 of tunnels after explosions. Major findings from two studies (Koneshwaran, et al., 2015d, Yang, et
 670 al., 2019) using different crack indexes to establish the damage criterion (one is based on penetrating
 671 cracks and the other depends on the crack width and number) are listed in **Table 15**. The damage
 672 category based on crack grades was obtained qualitatively instead of quantitatively, which means the
 673 assessment could be subjective.

674 **Table 15** The damage levels of tunnel lining based on crack grades

Ref.	Damage level	Description
(Yang, et al., 2019)	Slight damage	No penetrating cracks, overall good performance of tunnel lining
	Moderate damage	Short penetrating cracks
	Severe damage	Penetrating cracks running through the whole lining wall
	Collapse	The coalescence of multiple penetrating cracks running through the whole lining wall
(Koneshwaran, et al., 2015d)	No damage	Some minor cracks in segments with maximum crack width < 0.3 mm, and no bolt failure
	Slight damage	A small number of cracks with maximum crack width > 0.3 mm, and a few bolts fail at the joints, but no significant drifting response
	Moderate damage	A large number of cracks with maximum crack width > 0.3 mm, a large number of failed bolts, and significant drifting or sliding of segments at joints, but remaining the functionality of tunnel
	Severe damage or collapse	Formation of full depth cracks, and a large number of bolt failures, resulting in a large drift between segments

675 **5.4 Based on moment-force interaction diagram**

676 The combination of axial forces and bending moments causing structure failure allows to
 677 determine the moment-force interaction curve (Rashiddel, et al., 2020). There are two methods to
 678 obtain the moment-force diagram for the damage assessment of tunnel structures in literature. The
 679 first method is to utilize the design codes of RC structure to calculate the moment- force diagram for

680 tunnel lining. As reported, Yu, et al. (2014) adopted GB50010-2010 (MOHURD, 2011) code and Gui
681 and Chien (2006) used ACI 318-99 (ACI, 1999) code to calculate the moment-force diagram of RC
682 wall, which was used as the moment-force interaction diagram of tunnel lining. For instance, the
683 critical moment-force equation of RC wall subjected to combined flexure and axial loads in ACI 318-
684 99 is given as Eq. (1). It should be noted that the moment-force diagram calculated from these design
685 codes does not consider the influences of the curvature of tunnel cross-section and the surroundings-
686 structure interaction on the capacity of tunnel lining. The second method to obtain the moment-force
687 diagram of tunnel lining was proposed by Colombo, et al. (2015, 2016). The moment-force interaction
688 diagram was built by evaluating the diagrams of bending moment versus curvature of the tunnel cross-
689 section for different axial forces and considering the peak of each curve in the diagram as the resistant
690 moment for a given axial force. However, the interaction between lining and surroundings was not
691 taken into account in establishing the moment-force interaction diagram. Further study should be
692 conducted to develop the moment-force interaction diagram by considering the surroundings-lining
693 interaction for road tunnel.

$$694 \quad M_{ua} = M_c \times (1 - 5P_u l_c^2 / (0.75 * 48E_c I_{cr})) \quad (1)$$

695 where M_c is the design moment strength of RC wall, M_{ua} and P_u are the moment and axial force
696 acting on wall, respectively. l_c is the height of wall, E_c is the modulus of elasticity of concrete, and
697 I_{cr} is the moment of inertia of wall section.

698 **5.5 Based on pressure-impulse diagram**

699 The pressure-impulse diagram can be used for the damage assessment of tunnel lining on the basis
700 of pre-defined damage criteria, such as the deflection-span ratio (Ma, et al., 2008, 2010) and the
701 moment-force interaction diagram (Colombo, et al., 2015). Based on the given damage criteria, a
702 group of pressure and impulse applying onto tunnel lining at the ultimate limit state could be obtained
703 for the critical pressure-impulse diagram. For instance, Ma, et al. (2008, 2010) generated the pressure-
704 impulse diagrams for different damage modes of lining walls under blast loads based on the maximum
705 shear and bending displacements, in which the governing equations of pressure-impulse diagram is
706 given in Eq. (2). In addition, Colombo, et al. (2015) built up the pressure-impulse diagram of tunnel
707 lining by using the moment-force interaction diagram, In that study, the moment-force interaction
708 diagram neglected the interaction between tunnel structure and surroundings, which might undermine
709 the accuracy of the established pressure-impulse diagram. Therefore, a reliable pressure-impulse
710 diagram should be developed by considering surroundings-tunnel interaction in the future.

$$\begin{cases} S(P^*, I^*) = 1.1 \times \delta h \gamma_v \\ B(P^*, I^*) = 1.2 L \beta \end{cases} \quad (2)$$

where δ is material parameter varying from 0.6 to 0.866, h is the thickness of lining, γ_v is the critical shear strain, L is the half length of lining, and β is the ratio of mid-span deflection to half span. $S(P^*, I^*)$ and $B(P^*, I^*)$ are the implicit expressions with respect to normalized pressure and impulse for shear and bending, respectively.

5.6 Based on charge weight versus standoff distance

The damage assessment can also be performed by using charge weight and standoff distance based on some pre-defined damage criteria, such as the deflection-span ratio (Yang, et al., 2019), the crack grades (Koneshwaran, 2014, Koneshwaran, et al., 2015d), and the moment-force diagram (Colombo, et al., 2016), etc. According to the given damage criteria, the damage level of tunnel structures can be obtained corresponding to the given charge weight and standoff distance. Based on the obtained damage level under the specific charge weight and standoff distance, the boundary lines between different damage levels are fitted in the diagram of charge weight versus standoff distance. Threshold equations from Yang, et al. (2019) for different damage levels are given in Eq. (3). It is noted that in addition to the charge weight and standoff distance, there are some other factors as discussed in Section 4.3 influencing the damage levels of tunnel under blast loads. Therefore, this damage criterion should be cautiously used while other influencing factors might be involved.

$$R = \begin{cases} 3.27 \ln(W) - 5.82 & \text{Slight damage} \\ 4.05 \ln(W) - 10.80 & \text{Moderate damage} \\ 4.14 \ln(W) - 13.81 & \text{Severe damage} \end{cases} \quad (2m \leq R \leq 8m) \quad (3)$$

where R is the standoff distance (m); W is the charge weight in TNT equivalence (kg).

5.7 Based on empirical equation of spall and breach

An empirical approach in UFC 3-340-02 (US Department of Defense, 2008), which was derived to calculate spalling and breaching in concrete slabs under blast loading, has been used to evaluate blast damage of tunnel lining by Bai, et al. (2018). The expressions of the empirical equation is given as

$$\frac{h}{R} = \begin{cases} \frac{1}{a_1 + b_1 \psi^{2.5} + c_1 \psi^{0.5}} & \text{Spall threshold} \\ \frac{1}{a_2 + b_2 \psi + c_2 \psi^2} & \text{Breach threshold} \end{cases} \quad (4)$$

736 where h is the damaged concrete thickness (ft); R is the standoff distance from slab to charge centre
737 (ft), a_1 , b_1 , c_1 are constants equal to 20.02511, 0.01004, and 0.13613, respectively; and a_2 , b_2 , c_2 are
738 equal to 0.028205, 144308, and 0.049265, respectively. Ψ is a spall parameter related to the concrete
739 compressive strength, steel weight, and charge weight. The details can be referred to UFC 3-340-02
740 (US Department of Defense, 2008) and Bai, et al. (2018). Based on the empirical equation, the extent
741 of spalling and breaching damage of tunnel lining could be determined under different charge weights.
742 It should be noted that the empirical approach is established for free air or surface bursts. The multiple
743 interactions between blast wave and tunnel structures are not considered. In addition, this method
744 neglects the interaction between lining and surroundings.

745 **6. Damage mitigation measures of tunnel under explosion**

746 A range of mitigation measures against explosions has been developed, which could be classified
747 into two categories, i.e., active and passive measures. The active mitigation measures reduce the
748 destructive effects on tunnels by controlling the explosion source or activating appropriate systems
749 to minimize blast pressure and impulse acting on tunnel structures. The passive mitigation measures
750 mitigate blast damage to tunnel by installing protective layers, using high performance lining
751 materials, and changing components of tunnels, etc.

752 **6.1 Active mitigation measures**

753 Tunnel structures usually face three main threats of explosion sources, i.e., terrorist attacks (i.e.
754 high explosive), explosions of dangerous transported goods (i.e. VCE or BLEVE), and adjacent
755 construction blasts (i.e. high explosive). The terrorist attacks are conducted intentionally by terrorists
756 or hostile forces, while VCEs or BLEVEs accidentally occur in tunnels. The locations of such
757 explosions vary and are difficult to be predicted. However, the threats of engineering blasting for
758 construction near tunnels can be actively mitigated by controlling the explosion source. The designers
759 of engineering blasting can adjust the blasting parameters to control blast pressure from explosion
760 source, e.g., by using the millisecond delay technique (Qiu, 2014) and decoupling charge structures
761 (Park and Jeon, 2010). The technique of millisecond delay could reduce blast pressures by controlling
762 the delay times among a series of explosions. The decoupling charge structures could reduce the
763 detonation pressures transmitting into soil or rock.

764 Apart from controlling the explosion source itself, suppression systems to reduce blast pressures
765 in tunnel can be adopted to mitigate the damage of tunnel structures if the initiation of explosion is
766 unavoidable (Shirbhate and Goel, 2020). A representative automatic suppression system is the high-

767 speed, long-acting water deluge system, which has been used to mitigate the explosion threats in
 768 underground facilities (Chikhradze, et al., 2017). It is noted that an appropriate active suppression
 769 system must have a quick trigger, otherwise the shock wave that propagates rapidly in the tunnel
 770 cannot be suppressed in time. Although some active protection measures are currently available, their
 771 effectiveness and applicability are not necessarily assured since the explosions tend to be intensive
 772 and the blast waves propagate in sonic or supersonic velocities.

773 6.2 Passive mitigation measures

774 Compared to the active mitigation measures, the passive mitigation measures of tunnels against
 775 explosion loads have been more widely studied due to their adaptability to various explosion
 776 scenarios. Existing passive mitigation measures for tunnels can be divided into three categories, i.e.,
 777 changing components of tunnel itself, installing protective measures, and using high performance
 778 materials. **Table 16** summarizes various mitigation and reinforcement measures for each category
 779 and their corresponding working mechanisms, and effectiveness and cost of specific measures.

780 **Table 16.** Summary of three passive measures.

Categories	Types	Specific measures	Mechanism	Effectiveness	Cost
Changing components of tunnel itself	Reinforcement	Anchoring	Improving strength of rock/soil surroundings	High	Moderate
		Grouting	Enhancing strength of soil surroundings	High	Moderate
		Increasing lining thickness and concrete grade	Enhancing strength and stiffness of lining	High	Moderate
	Mitigation	Providing ventilation channels	Releasing blast waves to outside of the tunnel	Moderate	High
		Using flexible joint bolts for segment lining	Increasing allowance of lining deformation.	Moderate	Moderate
Installing protective measures	Reinforcement	Applying CFRP sheet	Improving flexural rigidity and tensile capacity of tunnel lining	High	Moderate
	Mitigation	Applying polyurethane foam, expandable polystyrene (EPS) foam, wood, rubber, EPS-cement matrix, and protective steel sheets	Enhancing blast energy absorption	High	Moderate
Using high-performance materials	Reinforcement	Fiber-reinforced concrete	Improving the tensile and post-peak performance of lining.	High	High
	Mitigation	Sandwich structures	Enhancing blast energy-absorbing capability	High	High

781 The components of tunnel can be changed and enhanced by (1) installing some support measures
 782 such as anchoring (Deng, et al., 2014, Wu, et al., 2011) and grouting (Liu, 2009), (2) providing
 783 ventilation channels (Han, 2014, Tiwari, et al., 2015, Van den Berg and Weerheijm, 2006), (3)
 784 adjusting the parameters of the structure itself such as increasing the lining thickness (Tiwari, et al.,
 785 2015, 2018), improving the concrete grade of tunnel lining (Tiwari, et al., 2018), enhancing the steel

786 reinforcement (Yang, et al., 2019), using the flexible joint bolts for the segment lining (Zhao, et al.,
787 2016), and adding the flexible honeycomb between the segments (Koneshwaran, 2014). The
788 anchoring could strengthen the inner connection of tunnel surroundings to improve the stability of
789 tunnel surroundings, while the grouting can enhance the strength and stiffness of soil surroundings to
790 significantly increase the blast-resistance of tunnel structures. Installing the ventilation channels can
791 release the blast wave inside the tunnel to outside of the tunnel, thereby reducing the range and level
792 of tunnel damage. The parameter-adjusting measures, such as increasing the thickness, concrete grade,
793 and steel reinforcement of tunnel lining could enhance the strength and stiffness of structure, while
794 other measures such as using flexible joint bolts for segment lining and adding flexible honeycomb
795 between segments could increase the allowance of lining deformation against blast loading.

796 Installing protective layers on the surface or in the vicinity of tunnel is another effective mitigation
797 measure. The polyurethane foam (De, et al., 2016, Koneshwaran, 2014), the expandable polystyrene
798 (EPS) foam (Qiu, 2014), the wood (Qiu, 2014), the rubber (Qiu, 2014), the EPS-cement matrix (Zhao,
799 et al., 2015), and the protective steel sheets (Cichocki, 1999) have been studied as the sacrificial
800 cladding or energy absorbing layer of tunnels. These materials installed on the surface or in the
801 vicinity of the tunnel could absorb blasting energy due to their high damping and compressibility
802 (Stolz, et al., 2010), which considerably reduces the intensity of blast loading acting on the tunnel
803 structure behind the protective layers. In addition to absorbing energy, the protective layers adhered
804 or wrapped on the tunnel lining using CFRP (Chen, et al., 2015, Xie, et al., 2014, Yang, et al., 2019)
805 can improve the flexural rigidity and loading capacity of tunnel lining, and suppress the formation of
806 structural cracks and the rotation of lining walls (Chen, et al., 2015, Xie, et al., 2014, Yang, et al.,
807 2019). It is worth noting that optimizing the thickness of protective layer is imperative for the
808 protective design of tunnel lining. A suitable thickness of protective layer can achieve good blast
809 resistance, beyond which the increase in thickness does not result in the incremental benefit.

810 In addition, high performance lining material can be used to replace traditional RC lining material
811 to improve the blast resistance of tunnels. Existing studies have experimentally and numerically
812 investigated the performance of tunnel linings made of advanced materials or structures, such as the
813 reinforced cement concrete (RCC) (Chaudhary, et al., 2018), the basalt fiber reinforced polymer
814 (BFRP) concrete (Zhou, et al., 2020), the steel fiber reinforced concrete (SFRC) (Chakrabortya, et al.,
815 2014, Chaudhary, et al., 2018), the high-performance fibre-reinforced cementitious composite
816 (HPFRCC) with the core of SFRC (Colombo, et al., 2014, 2015, 2016), the steel fibre reinforced
817 geopolymer concrete (SFRGC) (Meng, et al., 2020a, 2020b), the steel-dytherm foam-steel (SDS)
818 panel (Chakrabortya, et al., 2014, Chaudhary, et al., 2018), the steel polyurethane foam-steel (SPS)

819 panel (Chakrabortya, et al., 2014, Chaudhary, et al., 2018), and the steel-aluminium cenosphere
820 syntactic foam-steel (SAS) (Chaudhary, et al., 2018). It should be noted that although the high
821 performance materials have been intensively studied, their engineering application as lining material
822 is very limited due to the cost and immature construction technology. Therefore, the cost-
823 effectiveness and simplicity of these mitigation measures can be further investigated for engineering
824 practice.

825 **7. Future perspectives and conclusion**

826 This study presents a state-of-the-art review on the dynamic response, damage assessment and
827 damage mitigation of tunnel subjected to blast loads. Most relevant literatures regarding blast
828 response of tunnels have been reviewed to better understand the behaviors of road tunnels under blast
829 loads. Firstly, the common road tunnels, various explosion scenarios to tunnels, and the corresponding
830 blast wave characteristics around tunnel are reviewed. Next, the dynamic response and damage of
831 tunnel under blast loads, with respect to analysis methods of tunnel response, types of tunnel response,
832 and key factors influencing tunnel response are included. Then, the assessment criteria of tunnel
833 damage are summarized followed by the damage mitigation measures for tunnels against blast loads.
834 The main findings are summarized as follows.

835 (1) The existing theoretical methods to predict response of tunnel are not accurate enough due to
836 its elastic response assumption. Most of the existing experimental tests and numerical studies focused
837 on the tunnel response under high explosive explosions. Very limited studies investigated dynamic
838 response of tunnel under gas explosions and no study investigated dynamic response of tunnel caused
839 by the coupling effect of gas explosion and followed fire, which are deemed necessary for further
840 study.

841 (2) The existing experiments were carried out for tunnels in solid medium, while no published
842 experimental study on the response of tunnel in water has been conducted. In the previous numerical
843 studies on the dynamic response of tunnel in water, the effect of oscillations of water bubbles on
844 tunnel damage was not considered, leading to conservative estimation of the tunnel damage. Hence,
845 more studies are required to investigate dynamic response of tunnel in different buried media under
846 various types of explosions.

847 (3) Road tunnels could have different damage modes under different explosion conditions, i.e.,
848 the spalling and crushing of lining, cracks of lining, deformation and collapse of lining, bending and
849 tensile failure of reinforcement, and deformation and damage of tunnel surroundings. Most of the
850 existing studies focused on the blast damage to main structure (i.e., the lining) and surroundings. Only

851 limited studies investigated the blast damage to tunnel associated (i.e., secondary) structure, such as
852 the escape passage, the smoke channel, and the mid-wall of multi-cell tunnel. It should be noted the
853 associated structures of tunnel are more vulnerable to blast loads due to the lack of support from
854 surroundings. Hence, it is essential to investigate the dynamic response of the associated structures
855 and their influence on the damage behaviors of tunnels under blast loading in the future.

856 (4) The explosions occurring in the shallow buried road tunnel could induce ground vibrations
857 due to the intensive blast-induced stress wave, which might endanger adjacent buildings. Hence, the
858 performance and safety of buildings subjected to the tunnel explosion induced ground vibration need
859 be investigated for further study.

860 (5) Various influencing factors on the blast response of tunnel have been investigated. However,
861 some factors such as charge position insider and outside tunnel, tunnel cross sectional geometry and
862 dimension, depth ranges of shallow tunnel and deep tunnel, different slopes of tunnel, and interface
863 properties between lining and surroundings, have not been well investigated and are recommended
864 for further study.

865 (6) Various assessment methods of blast damage of tunnel have been proposed while these
866 methods have various limitations in assessing and quantifying blast damage of tunnel. Hence, there
867 remains a need for further study to develop reliable assessment methods to address these drawbacks
868 in the existing methods.

869 (7) A range of mitigation measures against blast damage of tunnel have been investigated.
870 However, most of the mitigation measures are still at the early research stage and have not be put into
871 engineering practice due to the high-cost and immature construction technology. There remains a
872 need for efficient, low-cost and easy-to-install mitigation measures for tunnels against blast loads.

873 **Acknowledgements**

874 The authors acknowledge the financial support from the Australian Research Council (ARC) via
875 Australian Laureate Fellowship (FL180100196).

876 **Reference**

- 877 AASHTO, A., 2012. A policy on geometric design of highways and streets. American Association of State Highway and
878 Transportation Officials. GDHS-6.
879 ACI, 1999. Building code requirements for structural concrete and commentary. American Concrete Institute. ACI 318-
880 99.
881 Al-Damluji, O.A.F.S., Al-Sa'aty, A.Y.T., Al-Nu'aimy, R.M.S., 2010. Effects of Internal Gas Explosion on an Underwater
882 Tunnel Roof. Fifth International Conferences on Recent Advances in Geotechnical Earthquake Engineering and Soil
883 Dynamics. San Diego, California, America.
884 Ansell, A., 1999. Dynamically loaded rock reinforcement. Royal Institute of Technology.

885 ASCE, 2011. Blast protection of buildings. American Society of Civil Engineers. ASCE/SEI 59-11
886 Auboyer, A., Andersen, V.,Wybo, J.L., 2007. State-of-the-art road tunnel safety. International Journal of Emergency
887 Management. 4 (4), 610-629
888 Austroads, 2019. Guide to Road Tunnels Part 2: Planning, Design and Commissioning Austroads. AGRT02-19.
889 Bai, F., Guo, Q., Root, K., Naito, C.,Quiel, S., 2018. Blast Vulnerability Assessment of Road Tunnels with Reinforced
890 Concrete Liners. Transp. Res. Rec. 2672 (41), 156-164
891 Bangash, M.Y.H.,Bangash, T., 2005. Explosion-resistant buildings: design, analysis, and case studies. Springer Science
892 & Business Media.
893 Bassan, S., 2015. Sight distance and horizontal curve aspects in the design of road tunnels vs. highways. Tunn. Undergr.
894 Space Technol. 45, 214-226
895 Birk, A.M., Davison, C.,Cunningham, M., 2007. Blast overpressures from medium scale BLEVE tests. J. Loss Prev.
896 Process Ind. 20 (3), 194-206
897 Birk, A.M., 2017. Shock waves and condensation clouds from industrial BLEVEs and VCEs. Process Saf. Environ. Prot.
898 110, 15-20
899 BTSICE, 2004. Tunnel lining design guide. The British Tunnelling Society and the Institution of Civil Engineers.
900 Buonsanti, M.,Leonardi, G., 2013. 3-D simulation of tunnel structures under blast loading. Arch. Civ. Mech. Eng. 13 (1),
901 128-134
902 CCPS, 2010. Guidelines for vapor cloud explosion, pressure vessel burst, bleve, and flash fire hazards. Center for
903 Chemical Process Safety.
904 Chakrabortya, T., Larcherb, M.,Gebbekenc, N., 2014. Performance of tunnel lining materials under internal blast loading.
905 Int. J. Prot. Struct. 5 (1), 83-96
906 Chaudhary, R.K., Mishra, S., Chakraborty, T.,Matsagar, V., 2018. Vulnerability analysis of tunnel linings under blast
907 loading. Int. J. Prot. Struct. 10 (1), 73-94
908 Chen, H.-L., Jin, F.-N.,Fan, H.-L., 2013a. Elastic responses of underground circular arches considering dynamic soil-
909 structure interaction: A theoretical analysis. Acta. Mech. Sin. 29 (1), 110-122
910 Chen, H., Zhou, J., Fan, H., Jin, F., Xu, Y., Qiu, Y., Wang, P.,Xie, W., 2014. Dynamic responses of buried arch structure
911 subjected to subsurface localized impulsive loading: Experimental study. Int. J. Impact Eng. 65, 89-101
912 Chen, H., Xie, W., Jiang, M., Wang, P., Zhou, J., Fan, H., Zheng, Q.,Jin, F., 2015. Blast-loaded behaviors of severely
913 damaged buried arch repaired by anchored CFRP strips. Compos. Struct. 122, 92-103
914 Chen, H.L., Xia, Z.C., Zhou, J.N., Fan, H.L.,Jin, F.N., 2013b. Dynamic responses of underground arch structures
915 subjected to conventional blast loads: Curvature effects. Arch. Civ. Mech. Eng. 13 (3), 322-333
916 Chikhradze, N., Mataradze, E., Chikhradze, M., Krauthammer, T., Mansurov, Z.,Alyiev, E., 2017. Methane Explosion
917 Mitigation in Coal Mines by Water Mist. IOP Conference Series: Earth and Environmental Science.
918 Choi, S., Wang, J., Munfakh, G.,Dwyre, E., 2006. 3D nonlinear blast model analysis for underground structures.
919 GeoCongress 2006: Geotechnical Engineering in the Information Technology Age. GeoCongress 2006: Geotechnical
920 Engineering in the Information Technology Age.
921 Cichocki, K., 1999. Effects of underwater blast loading on structures with protective elements. Int. J. Impact Eng. 22
922 (1999), 609-617
923 Colombo, M., Martinelli, P.,di Prisco, M., 2014. On the blast resistance of high performance tunnel segments. Mater.
924 Struct. 49 (1-2), 117-131
925 Colombo, M., Martinelli, P.,di Prisco, M., 2015. A design approach for tunnels exposed to blast and fire. Struct. Concr.
926 16 (2), 262-272
927 Colombo, M., Martinelli, P.,di Prisco, M., 2016. Underground Tunnels Exposed to Internal Blast: Effect of the Explosive
928 Source Position. Key Eng. Mater. 711, 852-859
929 Cui, X., Li, S., Lou, J., Wang, Z., Zhang, J., Tang, W.,Gao, Z., 2015. Dynamic responses and damage analyses of tunnel
930 lining and errant large vehicle during collision. Tunn. Undergr. Space Technol. 50, 1-12
931 Dang, V.K., Dias, D., Do, N.A.,Vo, T.H., 2018. Impact of Blasting at Tunnel Face on an Existing Adjacent Tunnel. Int.
932 J. GEOMATE. 15 (47), 22-31
933 De, A., Morgante, A.N.,Zimmie, T.F., 2013. Mitigation of blast effects on underground structure using compressible
934 porous foam barriers. In Poromechanics V: Proceedings of the Fifth Biot Conference on Poromechanics.
935 De, A., Morgante, A.N.,Zimmie, T.F., 2016. Numerical and physical modeling of geofam barriers as protection against
936 effects of surface blast on underground tunnels. Geotext. Geomembr. 44 (1), 1-12
937 De, A., Niemiec, A.,Zimmie, T.F., 2017. Physical and Numerical Modeling to Study Effects of an Underwater Explosion
938 on a Buried Tunnel. J. Geotech. Geoenviron. Eng. 143 (5), 04017002
939 Deng, X., Wang, J., Wang, R.,Liu, Q., 2020. Influence of Blasting Vibrations Generated by Tunnel Construction on an
940 Existing Road. International Journal of Civil Engineering. 18 (12), 1381-1393
941 Deng, X.F., Zhu, J.B., Chen, S.G., Zhao, Z.Y., Zhou, Y.X.,Zhao, J., 2014. Numerical study on tunnel damage subject to
942 blast-induced shock wave in jointed rock masses. Tunn. Undergr. Space Technol. 43, 88-100

943 Dhamne, R., Mishra, S., Kumar, A., Rao, K.S., 2018. Numerical study of the cross-sectional shape of shallow tunnels
944 subjected to impact and blast loading. National Conference On Prospects & Retrospect in Engineering Geology,
945 Geophysics & Instrumentation.

946 Dix, A., 2012. Tunnel fire investigation III: the Burnley Tunnel fire. In Handbook of Tunnel Fire Safety. 2007.03.27
947 Dowding, C.H., 1984. Estimating earthquake damage from explosion testing of full-scale tunnels. Adv. Technol.
948 Subsurf. Use. 4 (3), 113-117

949 DTMR, 2020. Design Criteria for Bridges and Other Structures Department of Transport and Main Roads.

950 Duan, B., Xia, H., Yang, X., 2018. Impacts of bench blasting vibration on the stability of the surrounding rock masses of
951 roadways. Tunn. Undergr. Space Technol. 71, 605-622

952 Feldgun, V.R., Kochetkov, A.V., Karinski, Y.S., Yankelevsky, D.Z., 2008. Blast response of a lined cavity in a porous
953 saturated soil. Int. J. Impact Eng. 35 (9), 953-966

954 Feldgun, V.R., Karinski, Y.S., Yankelevsky, D.Z., 2013a. The effect of an intermediate inclusion in soil on a buried lined
955 tunnel due to a nearby explosion Int. J. Prot. Struct. 4 (1), 1-20

956 Feldgun, V.R., Karinski, Y.S., Yankelevsky, D.Z., 2013b. A coupled approach to simulate the explosion response of a
957 buried structure in a soil-rock layered medium Int. J. Prot. Struct. 4 (3), 231-292

958 Feldgun, V.R., Karinski, Y.S., Yankelevsky, D.Z., 2014. The effect of an explosion in a tunnel on a neighboring buried
959 structure. Tunn. Undergr. Space Technol. 44, 42-55

960 Gao, M., Wang, Y., Gao, G.Y., Yang, J., 2013. An analytical solution for the transient response of a cylindrical lined
961 cavity in a poroelastic medium. Soil Dyn. Earthq. Eng. 46, 30-40

962 Gebbeken, N., Döge, T., 2010. Explosion Protection—Architectural Design, Urban Planning and Landscape Planning. Int.
963 J. Prot. Struct. 1 (1), 1-21

964 Goel, M.D., Verma, S., Panchal, S., 2020. Effect of Internal Blast on Tunnel Lining and Surrounding Soil. Indian Geotech.
965 J., 10.1007/s40098-020-00451-1,

966 Groethe, M., Merilo, E., Colton, J., Chiba, S., Sato, Y., Iwabuchi, H., 2007. Large-scale hydrogen deflagrations and
967 detonations. Int. J. Hydrog. Energy. 32 (13), 2125-2133

968 Gui, M.W., Chien, M.C., 2006. Blast-resistant Analysis for a Tunnel Passing Beneath Taipei Shongsan Airport—a
969 Parametric Study. Geotech. Geol. Eng. 24 (2), 227-248

970 Han, Y., 2014. Mechanism of saturated ground-tunnel interaction under medium blast loading. The city College of New
971 York.

972 Han, Y., Zhang, L., Yang, X., 2016. Soil-tunnel Interaction under Medium Internal Blast Loading. Procedia Eng. 143,
973 403-410

974 Hao, H., Wu, C., 2001. Scaled-Distance Relationships For Chamber Blast Accidents in Underground Storage of
975 Explosives. Fragblast. 5 (1-2), 57-90

976 Hao, H., 2015. Predictions of structural response to dynamic loads of different loading rates. Int. J. Prot. Struct. 6, 585-
977 605

978 Hao, H., Hao, Y., Li, J., Chen, W., 2016. Review of the current practices in blast-resistant analysis and design of concrete
979 structures. Adv. Struct. Eng. 19 (8), 1193-1223

980 He, S., Su, L., Fan, H., Ren, R., 2019. Methane explosion accidents of tunnels in SW China. Geomat. Nat. Haz. Risk. 10
981 (1), 667-677

982 Hendron, A.J., 1978. Engineering of rock blasting on civil projects. Int. J. Rock Mech. Min. Sci. Geomech. Abstr. 15 (3),
983 66

984 Higgins, W., Chakraborty, T., Basu, D., 2013. A high strain-rate constitutive model for sand and its application in finite-
985 element analysis of tunnels subjected to blast. Int. J. Numer. Anal. Methods Geomech. 37 (15), 2590-2610

986 Ingason, H., Li, Y.Z., 2017. Spilled liquid fires in tunnels. Fire Saf. J. 91, 399-406

987 Jiang, N., Zhou, C., 2012. Blasting vibration safety criterion for a tunnel liner structure. Tunn. Undergr. Space Technol.
988 32, 52-57

989 Joachim, C.E., 1990. Shallow underground tunnel/chamber explosion test program summary report. Army Engineer
990 Waterways Experiment Station Vicksburg Ms Structures Lab. SL-90-10.

991 JRA, 2003. Technical Standard for Structure Design of Road Tunnel. Japan Road Association.

992 Khan, S., Chakraborty, T., Matsagar, V., 2016. Parametric Sensitivity Analysis and Uncertainty Quantification for Cast
993 Iron-Lined Tunnels Embedded in Soil and Rock under Internal Blast Loading. J. Perform. Constr. Facil. 30 (6),
994 Kiger, S.A., Dallriva, F.D., Hall, R.L., 1989. Dynamic skin-friction effects on buried arches. J. Struct. Eng. 115 (7), 1768-
995 1781

996 Koneshwaran, S., Thambiratnam, D.P., Gallage, C., 2013. Response of a Buried Tunnel to Surface Blast using Different
997 Numerical Techniques. Proceedings of the Fourteenth International Conference on Civil, Structural and Environmental
998 Engineering Computing. Stirlingshire. Civil-Comp Press.

999 Koneshwaran, S., 2014. Blast response and sensitivity analysis of segmental tunnel Queensland University of Technology

1000 Koneshwaran, S., Thambiratnam, D.P., Gallage, C., 2015a. Performance of Buried Tunnels Subjected to Surface Blast
1001 Incorporating Fluid-Structure Interaction. J. Perform. Constr. Facil. 29 (3), 04014084

1002 Koneshwaran, S., Thambiratnam, D.P.,Gallage, C., 2015b. Blast Response of Segmented Bored Tunnel using Coupled
1003 SPH-FE Method. Structures. 2, 58-71
1004 Koneshwaran, S., Thambiratnam, D.P.,Gallage, C., 2015c. Response of segmented bored transit tunnels to surface blast.
1005 Adv. Eng. Softw. 89, 77-89
1006 Koneshwaran, S., Thambiratnam, D.P.,Gallage, C., 2015d. Blast Response and Failure Analysis of a Segmented Buried
1007 Tunnel. Struct. Eng. Int. 25 (4), 419-431
1008 Kristiansen, E.A., 2019. Submerged floating tunnels in concrete exposed to blast loading. Norwegian University of
1009 Science and Technology.
1010 Kristoffersen, M., Minoretta, A.,Børvik, T., 2019. On the internal blast loading of submerged floating tunnels in concrete
1011 with circular and rectangular cross-sections. Eng. Fail. Anal. 103, 462-480
1012 Krone, E., 2018. Internal Blast Loading of Submerged Floating Tunnels in Concrete. Norwegian University of Science
1013 and Technology.
1014 Lai, H., Wang, S.,Xie, Y., 2016. Study on the Fire Damage Characteristics of the New Qidaoliang Highway Tunnel: Field
1015 Investigation with Computational Fluid Dynamics (CFD) Back Analysis. Int. J. Environ. Res. Public Health. 13 (10),
1016 1014
1017 Li, C.,Li, X., 2018. Influence of wavelength-to-tunnel-diameter ratio on dynamic response of underground tunnels
1018 subjected to blasting loads. Int. J. Rock Mech. Min. Sci. 112, 323-338
1019 Li, J.,Hao, H., 2020. Numerical study of medium to large scale BLEVE for blast wave prediction. J. Loss Prev. Process
1020 Ind. 65, 104107
1021 Li, J.,Hao, H., 2021. Numerical simulation of medium to large scale BLEVE and the prediction of BLEVE's blast wave
1022 in obstructed environment. Process Saf. Environ. Prot. 145, 94-109
1023 Li, X., Li, C., Cao, W.,Tao, M., 2018. Dynamic stress concentration and energy evolution of deep-buried tunnels under
1024 blasting loads. Int. J. Rock Mech. Min. Sci. 104, 131-146
1025 Li, Z.,Huang, H., 1994. The calculation of stability of tunnel under effects of seismic wave of explosion. Proceedings of
1026 26th Department of Defence Explosives Safety Seminar. Beijing.
1027 Li, Z., 2018. Study on damage mechanism and repair technology of tunnelling subjected to gas explosion. Beijing
1028 University of Science and Technology
1029 Li, Z., Wu, S., Cheng, Z.,Jiang, Y., 2018. Numerical Investigation of the Dynamic Responses and Damage of Linings
1030 Subjected to Violent Gas Explosions inside Highway Tunnels. Shock Vib. 2018, 1-20
1031 Li, Z., Tao, M., Du, K., Cao, W.,Wu, C., 2020. Dynamic stress state around shallow-buried cavity under transient P wave
1032 loads in different conditions. Tunn. Undergr. Space Technol. 97, 103228
1033 Liang, Q., Li, J., Li, D.,Ou, E., 2012. Effect of Blast-Induced Vibration from New Railway Tunnel on Existing Adjacent
1034 Railway Tunnel in Xinjiang, China. Rock Mech. Rock Eng. 46 (1), 19-39
1035 Liu, H., 2009. Dynamic Analysis of Subway Structures Under Blast Loading. Geotech. Geol. Eng. 27 (6), 699-711
1036 Liu, H., 2012. Soil-Structure Interaction and Failure of Cast-Iron Subway Tunnels Subjected to Medium Internal Blast
1037 Loading. J. Perform. Constr. Facil. 26 (5), 691-701
1038 Liu, H.,Nezili, S., 2016. Centrifuge Modeling of Underground Tunnel in Saturated Soil Subjected to Internal Blast
1039 Loading. J. Perform. Constr. Facil. 30 (2),
1040 Liu, Z., Jiang, N., Sun, J., Xia, Y.,Lyu, G., 2019. Influence of tunnel blasting construction on adjacent highway tunnel: A
1041 case study in Wuhan, China. Int. J. Prot. Struct. 11 (3), 283-303
1042 Lu, S., Zhou, C., Jiang, N.,Wu, C., 2016. Damage range caused by terrorist attacks in a double-track tunnel crossing under
1043 airport runway. Electron. J. Geotech. Eng. 21 (2016), 10457-10469
1044 Lu, Y., Wang, Z.,Chong, K., 2005. A comparative study of buried structure in soil subjected to blast load using 2D and
1045 3D numerical simulations. Soil Dyn. Earthq. Eng. 25 (4), 275-288
1046 Ma, G., Huang, X.,Li, J., 2008. Damage assessment for buried structures against internal blast load. Trans. Tianjin Univ.
1047 14 (5), 353-357
1048 Ma, G., Huang, X.,Li, J., 2010. Simplified damage assessment method for buried structures against external blast load. J.
1049 Struct. Eng. 136 (5), 603-612
1050 Ma, G., Zhou, H., Lu, Y.,Chong, K., 2010. In-structure shock of underground structures: A theoretical approach. Eng.
1051 Struct. 32 (12), 3836-3844
1052 Mandal, J., Agarwal, A.K.,Goel, M.D., 2020. Numerical Modeling of Shallow Buried Tunnel Subject to Surface Blast
1053 Loading. J. Perform. Constr. Facil. 34 (6), 04020106
1054 Masellis, M., laia, A., Sferrazza, G., Pirillo, E., D'Arpa, N., Cucchiara, P., Sucameli, M., Napoli, B., Alessandro,
1055 G.,Gaiarmi, S., 1997. Fire disaster in a motorway tunnel. Ann. Burn. Fire Disasters. 10 (4), 1-11
1056 McDaniel, K.H., 2017. A new methodology to evaluate critical fire life safety and emergency preparedness in vehicular
1057 road tunnels. Colorado School of Mines.
1058 Meng, Q., Wu, C., Hao, H., Li, J., Wu, P., Yang, Y.,Wang, Z., 2020a. Steel fibre reinforced alkali-activated geopolymer
1059 concrete slabs subjected to natural gas explosion in buried utility tunnel. Constr. Build. Mater. 246,

1060 Meng, Q., Wu, C., Li, J., Liu, Z., Wu, P., Yang, Y., Wang, Z., 2020b. Steel/basalt rebar reinforced Ultra-High Performance
1061 Concrete components against methane-air explosion loads. *Compos. B. Eng.* 198, 108215
1062 Mishra, S., Chakraborty, T., Basu, D., Lam, N., 2020. Characterization of Sandstone for Application in Blast Analysis of
1063 Tunnel. *Geotech. Test J.* 43 (2), 351-382
1064 Mishra, S., Kumar, A., Rao, K.S., Gupta, N.K., 2020. Experimental and numerical investigation of the dynamic response
1065 of tunnel in soft rocks. *Structures.* 10.1016/j.istruc.2020.08.055,
1066 Mitelman, A., Elmo, D., 2014. Modelling of blast-induced damage in tunnels using a hybrid finite-discrete numerical
1067 approach. *J. Rock Mech. Geotech. Eng.* 6 (6), 565-573
1068 Mitelman, A., Elmo, D., 2016. Analysis of tunnel support design to withstand spalling induced by blasting. *Tunn. Undergr.*
1069 *Space Technol.* 51, 354-361
1070 Mo, Y., Teng, B., Zou, Z.Y., Li, L., Zhong, M., 2013. Small Spacing Tunnels the Blasting Excavation Dynamic Effect.
1071 *Appl. Mech. Mater.* 353, 1484-1489
1072 Mobaraki, B., Vaghefi, M., 2015. Numerical study of the depth and cross-sectional shape of tunnel under surface explosion.
1073 *Tunn. Undergr. Space Technol.* 47, 114-122
1074 Mobaraki, B., Vaghefi, M., 2016. Effect of the soil type on the dynamic response of a tunnel under surface detonation.
1075 *Combust. Explos. Shock Waves.* 52 (3), 363-370
1076 MOHURD, 2011. Chinese code for design of concrete structures. Ministry of Housing and Urban-Rural Development of
1077 the People's Republic of China.
1078 Molenaar, D.J., Weerheijm, J., Vervuurt, A., Burggraaf, H., Roekaerts, D., Meijers, P., 2009. Bijzondere belastingen in
1079 tunnels: Eindrapport. TC211-05-09.
1080 MTPRC, 2018. Specifications for design of highway tunnels section 1. Civil engineering. Ministry of Transport of the
1081 People's Republic of China. JTG 3370.1-2018.
1082 MTPRC, 2020. 2019 statistical bulletin of transportation industry development. Ministry of Transport of the People's
1083 Republic of China. 2020.05.12
1084 Mussa, M., Mutalib, A., Hamid, R., Raman, S., 2018. Blast Damage Assessment of Symmetrical Box-Shaped
1085 Underground Tunnel According to Peak Particle Velocity (PPV) and Single Degree of Freedom (SDOF) Criteria.
1086 *Symmetry.* 10 (5), 158
1087 Mussa, M.H., Mutalib, A.A., Hamid, R., Naidu, S.R., Radzi, N.A.M., Abedini, M., 2017. Assessment of damage to an
1088 underground box tunnel by a surface explosion. *Tunn. Undergr. Space Technol.* 66, 64-76
1089 Nagao, M., Takatori, T., Oono, T., Iwase, H., Iwadate, K., Yamada, Y., Nakajima, M., 1997. Death due to a methane gas
1090 explosion in a tunnel on urban reclaimed land. *Am. J. Forensic Med. Pathol.* 18 (2), 135-139
1091 NPRA, 2004. Road tunnel. Norwegian Public Road Administration. Manual 21.
1092 Osinov, V.A., Chrisopoulos, S., Triantafyllidis, T., 2019. Numerical analysis of the tunnel-soil interaction caused by an
1093 explosion in the tunnel. *Soil Dyn. Earthq. Eng.* 122, 318-326
1094 Park, D., Jeon, S., 2010. Reduction of blast-induced vibration in the direction of tunneling using an air-deck at the bottom
1095 of a blasthole. *Int. J. Rock Mech. Min. Sci.* 47 (5), 752-761
1096 Parviz, M., Aminnejad, B., Fiouz, A., 2017. Numerical simulation of dynamic response of water in buried pipeline under
1097 explosion. *KSCE J. Civ. Eng.* 21 (7), 2798-2806
1098 Prasanna, R., Boominathan, A., 2014. Response of tunnels due to blast loading. *Geotechnical Aspects of Underground*
1099 *Construction in Soft Ground.* Seoul, Korea. Korean Geotechnical Society.
1100 Prasanna, R., Boominathan, A., 2020. Finite-Element Studies on Factors Influencing the Response of Underground
1101 Tunnels Subjected to Internal Explosion. *Int. J. Geomech.* 20 (7), 04020089
1102 Prochazka, P., Jandeková, D., 2020. Effect of explosion source location on tunnel damage. *Int. J. Prot. Struct.*,
1103 10.1177/2041419620907924,
1104 Qiu, B., 2014. Numerical study on vibration isolation by wave barrier and protection of existing tunnel under explosions.
1105 *Laboratory of Civil and Environmental Engineering (LGCIE).*
1106 Rashidell, A., Kharghani, M., Dias, D., Hajihassani, M., 2020. Numerical study of the segmental tunnel lining behavior
1107 under a surface explosion – Impact of the longitudinal joints shape. *Comput. Geotech.* 128, 103822
1108 RDA, JICA, 2018. Guideline for design of road tunnel Road Development Authority (RDA) and Japan International
1109 Cooperation Agency (JICA).
1110 Roberts, J.E., Kulicki, J.M., Beranek, D.A., Englot, J.M., Fisher, J.W., Hungerbeeler, H., 2003. Recommendations for
1111 Bridge and Tunnel Security. American Association of State Highway and Transportation Officials (AASHTO) and
1112 Federal Highway Administration (FHWA).
1113 Senjuntichai, T., Rajapakse, R., 1993. Transient response of a circular cavity in a poroelastic medium *Int. J. Numer. Anal.*
1114 *Methods Geomech.* 17 (6), 357-383
1115 Shakeri, R., Mesgouez, A., Lefeuve-Mesgouez, G., 2020. Transient response of a concrete tunnel in an elastic rock with
1116 imperfect contact. *International Journal of Mining Science and Technology.* 30 (5), 605-612
1117 Shin, J.-H., Moon, H.-G., Chae, S.-E., 2011. Effect of blast-induced vibration on existing tunnels in soft rocks. *Tunn.*
1118 *Undergr. Space Technol.* 26 (1), 51-61

1119 Shirbhate, P.A.,Goel, M.D., 2020. A Critical Review of Blast Wave Parameters and Approaches for Blast Load Mitigation.
1120 Arch. Comput. Methods Eng., 10.1007/s11831-020-09436-y,
1121 Shirlaw, J.N., Hencher, S.R.,Zhao, J., 2000. Design and construction issues for excavation and tunnelling in some
1122 tropically weathered rocks and soils. In ISRM International Symposium. International Society for Rock Mechanics and
1123 Rock Engineering. Melbourne.
1124 Slawson, T.R., 1984. Dynamic shear failure of shallow-buried flat-roofed reinforced concrete structures subjected to blast
1125 loading. Army Engineer Waterways Experiment Station Vicksburg Ms Structures Lab. ADA14594.
1126 Smith, J.L., Betz, J.F.,Baird, G.T., 1986. KACHINA test series: Dynamic arch test three (dat-3) analysis report Air Force
1127 Weapons Lab. AFWL-TR-85-63.
1128 Soheyli, M.R., Akhaveissy, A.H.,Mirhosseini, S.M., 2016. Large-Scale Experimental and Numerical Study of Blast
1129 Acceleration Created by Close-In Buried Explosion on Underground Tunnel Lining. Shock Vib. 2016, 1-9
1130 Stamos, A.A.,Beskos, D.E., 1995. Dynamic analysis of large 3-D underground structures by the bem. Earthquake
1131 engineering & structural dynamics. 24 (6), 917-934
1132 Stolz, A., Riedel, W., Mayrhofer, C., Nöldgen, M.,Dörendahl, K., 2010. Tunnel Structures subjected to Explosions. 5th
1133 Future Security. Berlin, Germany.
1134 Stolz, A.,Ruiz-Ripoll, M.L., 2015. Experimental and Computational Characterization of Dynamic Loading and Structural
1135 Resistance of Tunnels in Blast Scenarios. Fire Technol. 52 (5), 1595-1618
1136 Swisdak Jr, M.M., 1978. Explosion effects and properties. Part II. Explosion effects in water. Naval Surface Weapons
1137 Center White Oak Lab Silver Spring Md.
1138 Tao, M., Li, Z., Cao, W., Li, X.,Wu, C., 2019. Stress redistribution of dynamic loading incident with arbitrary waveform
1139 through a circular cavity. Int. J. Numer. Anal. Methods Geomech. 43 (6), 1279-1299
1140 TCRP86/NCHRP525, 2006. Transportation security-Making transportation tunnels safe and secure. Transportation
1141 Research Board.
1142 Tener, R.K., 1964. Model study of a buried arch subjected to dynamic loading. Iowa State University Of Science and
1143 Technology.
1144 Tiwari, R., Chakraborty, T.,Matsagar, V., 2015. Dynamic analysis of curved tunnels subjected to internal blast loading.
1145 Advances in Structural Engineering New Delhi. Springer.
1146 Tiwari, R., Chakraborty, T.,Matsagar, V., 2015. Dynamic Analysis of Twin Tunnel Subjected to Internal Blast Loading.
1147 Advances in Structural Engineering. New Delhi. Springer.
1148 Tiwari, R., Chakraborty, T.,Matsagar, V., 2016. Dynamic Analysis of Tunnel in Weathered Rock Subjected to Internal
1149 Blast Loading. Rock Mech. Rock Eng. 49 (11), 4441-4458
1150 Tiwari, R., Chakraborty, T.,Matsagar, V., 2017. Dynamic Analysis of Tunnel in Soil Subjected to Internal Blast Loading.
1151 Geotech. Geol. Eng. 35 (4), 1491-1512
1152 Tiwari, R., Chakraborty, T.,Matsagar, V., 2018. Analysis of curved tunnels in soil subjected to internal blast loading.
1153 Acta Geotech. 15 (2), 509-528
1154 Townsend, F.C., Zalzman, S., Tabatabai, H., McVay, M.C., Bloomquist, D.,Gill, J.J., 1987. Centrifugal and Numerical
1155 Modeling of Buried Structures Subjected to Blast Loading. International Conference on the Interaction of Conventional
1156 Munitions with Protective Structures. Mannheim, Germany.
1157 UKHA, 2000. Design Manual for Roads and Bridges, Part 9, Section 2 of Volume 2, Design of Road Tunnels. UK
1158 Highways Agency. DN-STR-03015.
1159 US Department of Defense, 2008. Structures to resist the effects of accidental explosions. US Department of Defense.
1160 UFC 3-340-02.
1161 USDTFHA, 2004. FHWA Road Tunnel Design Guidelines U.S. Department of Transportation Federal Highway
1162 Administration FHWA-IF-05-023
1163 USDTFHA, 2009. Technical Manual for Design and Construction of Road Tunnels — Civil Elements U.S. Department
1164 of Transportation Federal Highway Administration FHWA-NHI-10-034
1165 Van den Berg, A.C.,Weerheijm, J., 2006. Blast phenomena in urban tunnel systems. J. Loss Prev. Process Ind. 19 (6),
1166 598-603
1167 Verma, A.K., Jha, M.K., Mantrala, S.,Sitharam, T.G., 2017. Numerical Simulation of Explosion in Twin Tunnel System.
1168 Geotech. Geol. Eng. 35 (5), 1953-1966
1169 Vervuurt, A.H.J.M., Galanti, F.M.B., Wubsi, A.J.,Van den Berg, A.C., 2007. Effect of explosions in tunnels-Preliminary
1170 assessment of the structural response. 2007-D-R0156/A.
1171 Vivek, P.,Sitharam, T.G., 2017. Sand ejecta kinematics and impulse transfer associated with the buried blast loading: A
1172 controlled laboratory investigation. Int. J. Impact Eng. 104, 85-94
1173 Vivek, P.,Sitharam, T.G., 2018. Laboratory scale investigation of stress wave propagation and vibrational characteristics
1174 in sand when subjected to air-blast loading. Int. J. Impact Eng. 114, 169-181
1175 Wang, G., Lu, W., Yang, G., Yan, P., Chen, M., Zhao, X.,Li, Q., 2020. A state-of-the-art review on blast resistance and
1176 protection of high dams to blast loads. Int. J. Impact Eng. 139, 103529

1177 Wang, S., Li, Z., Fang, Q., Yan, H., Chen, L., 2021. Performance of utility tunnels under gas explosion loads. *Tunn. Undergr. Space Technol.* 109, 103762

1178 Wang, X., Wang, M., Chen, J., Yan, T., Bao, Y., Chen, J., Qin, P., Li, K., Deng, T., Yan, G., 2020. Analysis of calculation of fresh-air demand for road tunnel ventilation design in China. *Tunn. Undergr. Space Technol.* 103, 103469

1179 Wang, Z., Lu, Y., Hao, H., Chong, K., 2005. A full coupled numerical analysis approach for buried structures subjected to subsurface blast. *Comput. Struct.* 83 (4-5), 339-356

1180 Weidlinger, P., Hinman, E., 1988. Analysis of underground protective structures *J. Struct. Eng.* 114 (7), 1658-1673

1181 Wu, C., Hao, H., 2006. Numerical prediction of rock mass damage due to accidental explosions in an underground ammunition storage chamber. *Shock Waves.* 15 (1), 43-54

1182 Wu, Z.S., Chen, G.Q., Zen, K., Kasama, K., Wang, D.L., 2011. Effect of Blasting on the Adjacent Underground Tunnels. *Appl. Mech. Mater.* 90, 1870-1878

1183 Xia, X., Li, H.B., Li, J.C., Liu, B., Yu, C., 2013. A case study on rock damage prediction and control method for underground tunnels subjected to adjacent excavation blasting. *Tunn. Undergr. Space Technol.* 35, 1-7

1184 Xie, W., Jiang, M., Chen, H., Zhou, J., Xu, Y., Wang, P., Fan, H., Jin, F., 2014. Experimental behaviors of CFRP cloth strengthened buried arch structure subjected to subsurface localized explosion. *Compos. Struct.* 116, 562-570

1185 Yan, D., Wu, Q., Li, T., Ren, Y., 2019. Investigation and Analysis on the Explosion Accident in the Mountain Tunnel. *J. Eng. Sci. Technol. Rev.* 12 (4), 152-159

1186 Yang, G., Wang, G., Lu, W., Zhao, X., Yan, P., Chen, M., 2018. Numerical modeling of surface explosion effects on shallow-buried box culvert behavior during the water diversion. *Thin-Walled Struct.* 133, 153-168

1187 Yang, G., Wang, G., Lu, W., Yan, P., Chen, M., 2019. Damage assessment and mitigation measures of underwater tunnel subjected to blast loads. *Tunn. Undergr. Space Technol.* 94, 103131

1188 Yang, Y., Xie, X., Wang, R., 2010. Numerical simulation of dynamic response of operating metro tunnel induced by ground explosion. *J. Rock Mech. Geotech. Eng.* 2 (4), 373-384

1189 Yankelevsky, D.Z., Karinski, Y.S., Feldgun, V.R., 2012. Recent studies on buried explosions in dry soils in proximity to buried structures. Taylor and Francis Group.

1190 Yu, H., Yuan, Y., Yu, G., Liu, X., 2014. Evaluation of influence of vibrations generated by blasting construction on an existing tunnel in soft soils. *Tunn. Undergr. Space Technol.* 43, 59-66

1191 Yu, H., Wang, Z., Yuan, Y., Li, W., 2015. Numerical analysis of internal blast effects on underground tunnel in soils. *Struct. Infrastruct. Eng.* 12 (9), 1090-1105

1192 Zhao, H.-b., Long, Y., Li, X.-h., Lu, L., 2015. Experimental and numerical investigation of the effect of blast-induced vibration from adjacent tunnel on existing tunnel. *KSCE J. Civ. Eng.* 20 (1), 431-439

1193 Zhao, H., Yu, H., Yuan, Y., Zhu, H., 2015. Blast mitigation effect of the foamed cement-base sacrificial cladding for tunnel structures. *Constr. Build. Mater.* 94, 710-718

1194 Zhao, J., Gong, Q.M., Eisenstein, Z., 2007. Tunnelling through a frequently changing and mixed ground: A case history in Singapore. *Tunn. Undergr. Space Technol.* 22 (4), 388-400

1195 Zhao, Y., Chu, C., Yi, Y., 2016. Study on an engineering measure to improve internal explosion resistance capacity of segmental tunnel lining structures. *J. Vibroengineering.* 18 (5), 2997-3009

1196 Zhou, Q., He, H., Liu, S., Chen, X., Tang, Z., Liu, Y., Qiu, Z., Li, S., Wang, H., Zhou, Y., Zhou, J., Fan, H., Jin, F., 2020. Blast resistance evaluation of urban utility tunnel reinforced with BFRP bars. *Def. Technol.*, 10.1016/j.dt.2020.03.015,

1197 Zhou, Y., 2011. Earthquakes as a rock dynamic problem and their effects on rock engineering structures. *Advances in Rock Dynamics and Applications.* London. Taylor and Francis Group.